NAVAL POSTGRADUATE SCHOOL
Monterey, California

THESIS

QUALITY FUNCTIONAL DEPLOYMENT AS A CONCEPTUAL AIRCRAFT DESIGN TOOL

by

Rendell Kheng Wah Tan

March 2000

Thesis Advisor: Conrad F. Newberry

Approved for public release; distribution is unlimited.

REPORT DOCUMENTATION PAGE

Form Approved OMB No. 0704-0188

1. AGENCY USE ONLY *(Leave blank)*	2. REPORT DATE	3. REPORT TYPE AND DATES COVERED
	March 2000	Master's Thesis

4. TITLE AND SUBTITLE
QUALITY FUNCTIONAL DEPLOYMENT AS A CONCEPTUAL AIRCRAFT DESIGN TOOL

5. FUNDING NUMBERS

6. AUTHOR(S)
Tan, Rendell Kheng Wah

7. PERFORMING ORGANIZATION NAME(S) AND ADDRESS(ES)
Naval Postgraduate School
Monterey, CA 93943-5000

8. PERFORMING ORGANIZATION REPORT NUMBER

9. SPONSORING / MONITORING AGENCY NAME(S) AND ADDRESS(ES)

10. SPONSORING/MONITORING AGENCY REPORT NUMBER

11. SUPPLEMENTARY NOTES
The views expressed in this thesis are those of the author and do not reflect the official policy or position of the Department of Defense or the U.S. Government.

12a. DISTRIBUTION / AVAILABILITY STATEMENT
Approved for public release; distribution unlimited.

12b. DISTRIBUTION CODE

13. ABSTRACT *(Maximum 200 words)*

Quality Functional Deployment (QFD) methodology was applied as a possible system integration tool for use during the conceptual configuration design phase of low speed High Altitude Long Endurance (HALE) UAVs. A four-level QFD model was used to identify important design variables and prioritize those that impact customer attributes. The customer attributes were deployed into performance parameters. The performance parameters were deployed into UAV part characteristics. The part characteristics were deployed into manufacturing processes. The manufacturing processes were deployed into process controls. Based on QFD, the research effort showed that to achieve the customer attributes of high endurance, range, cruise altitude and payload, the important performance parameters are low gross weight, low $C_{D,0}$, high $C_{L,max}$ and a low life cycle cost. The part characteristics considered for the conceptual HALE UAV configuration were maximum utilization of composites, thick airfoil (to increase fuel capacity), high wing fatigue strength and low wing sweep. To achieve the part characteristics, the manufacturing methods considered were autoclaving and filament winding for composites components; milling and precision forging were considered for aluminum alloy components. Manufacturing process controls were also identified. In each QFD matrix, the technical correlations "roof" provided an effective mechanism for comparing each design parameter against other design parameters in order to determine conflicting design requirements.

14. SUBJECT TERMS
Quality Function Deployment, Aircraft Design.

15. NUMBER OF PAGES
102

16. PRICE CODE

17. SECURITY CLASSIFICATION OF REPORT	18. SECURITY CLASSIFICATION OF THIS PAGE	19. SECURITY CLASSIFICATION OF ABSTRACT	20. LIMITATION OF ABSTRACT
Unclassified	Unclassified	Unclassified	UL

NSN 7540-01-280-5500

Standard Form 298 (Rev. 2-89)
Prescribed by ANSI Std 239-18

Approved for public release; distribution is unlimited

QUALITY FUNCTION DEPLOYMENT AS A CONCEPTUAL AIRCRAFT DESIGN TOOL

Rendell K. W. Tan
Major, Republic of Singapore Air Force
Bachelor in Mechanical Engineering, Nanyang Technological University, 1995

Submitted in partial fulfillment of the
requirements for the degree of

MASTER OF SCIENCE IN AERONAUTICAL ENGINEERING

from the

NAVAL POSTGRADUATE SCHOOL
March 2000

Author: _____
Rendell K. W. Tan

Approved by: _____
Conrad F. Newberry, Thesis Advisor

_____
Russell W. Duren, Second Reader

_____
Max F. Platzer, Chairman
Department of Aeronautics and Astronautics

ABSTRACT

Quality Functional Deployment (QFD) methodology was applied as a possible system integration tool for use during the conceptual configuration design phase of low speed High Altitude Long Endurance (HALE) UAVs. A four-level QFD model was used to identify important design variables and prioritize those that impact customer attributes. The customer attributes were deployed into performance parameters. The performance parameters were deployed into UAV part characteristics. The part characteristics were deployed into manufacturing processes. The manufacturing processes were deployed into process controls. Based on QFD, the research effort showed that to achieve the customer attributes of high endurance, range, cruise altitude and payload, the important performance parameters are low gross weight, low $C_{D,0}$, high $C_{L,max}$ and a low life cycle cost. The part characteristics considered for the conceptual HALE UAV configuration were maximum utilization of composites, thick airfoil (to increase fuel capacity), high wing fatigue strength and low wing sweep. To achieve the part characteristics, the manufacturing methods considered were autoclaving and filament winding for composites components; milling and precision forging were considered for aluminum alloy components. Manufacturing process controls were also identified. In each QFD matrix, the technical correlations "roof" provided an effective mechanism for comparing each design parameter against other design parameters in order to determine conflicting design requirements.

TABLE OF CONTENTS

LIST OF FIGURES

This page is intentionally left blank.

LIST OF TABLES

This page is intentionally left blank.

LIST OF SYMBOLS, ACROYMNS, AND/OR ABBREVIATIONS

$C_{D,0}$	Zero Lift Drag Coefficient
W/S	Wing Loading
NACA	National Advisory Committee for Aeronautics
$C_{L,max}$	Maximum Lift Coefficient
C_L	Lift Coefficient
M	Mach Number
AR	Aspect Ratio
C_D	Drag Coefficient
e	Oswald Efficiency Factor
v	Velocity
T	Thrust
T_{SL}	Thrust, Sea Level
TSFC	Thrust, Specific Fuel Consumption (Ct)
W_{TO}	Weight, Take-Off
ROM	Rough Order of Magnitude
W_1	Weight (without fuel)
E	Endurance
D	Drag
A_O	Availability
α	Installed Thrust Lapse
β	Instantaneous Weight Fraction
q	Dynamic Pressure
S	Wing Area
n	Load Factor
h	Altitude
Ldg	Landing
Sus-Turn	Sustained Turn
Svc	Service
t/c	Thickness Over Chord Ratio
λ	Taper Ratio
Δ	Wing Sweep (quarter chord)
C_t	Tip Chord
C_r	Root Chord
QFD	Quality Functional Deployment
ASI	American Supplier Institute
UAV	Uninhabited Aerial Vehicle
MTTR	Mean Time To Repair
MTBF	Mean Time Between Failures

ERM	Elastic Reservoir Molding
CNC	Computer Numerical Control
P/M	Powder Metallurgy
NDI	Non-Destructive Method

ACKNOWLEDGEMENT

The author would like to thank Professor Conrad F. Newberry and Professor Russ Duren for their guidance and patience in this thesis effort. Thank you for the countless times for your expertise and experience in helping me stay the course.

Many, many thanks and gratitude to my lovely wife, Wai Teng for her love, encouragement, prayers and support. My darling wife, you are my inspiration! My wife and I are so blessed with three lovely children, i.e., Michelle, Jonathan and Ariel. Our bedtime stories kept me in perspective! This degree is really a Family Joint Operation!

To God be the glory, honor and praise forever! For it is through His grace that I have come this far in my military career and His strength that has helped me overcome every challenge. "Nothing is impossible for my God."

This page is intentionally left blank.

I. INTRODUCTION

A classic story of the application of Quality Functional Deployment (QFD) would be the dramatic success of Toyota, now an automobile icon and benchmark of quality and reliability. The Toyota example is indeed indisputable testimony to the application of QFD to car design that has greatly exceeded customers' expectations [Ref. 5]. This chapter covers the purpose of the thesis and introduces the application of a Four-Level QFD model for aircraft conceptualization design.

A. PURPOSE OF THESIS

The purpose this thesis is to develop an approach for the application of the QFD methodology as a system integration tool during the conceptual design of a generic aircraft. The thesis will show how the customer attributes, i.e., operational requirements [based on Request for Proposal (RFP)] can be translated into conceptual design criteria. A QFD model was used to identify important design variables and prioritize those that are paramount to the aircraft mission.

B. THE FOUR-PHASE QFD MODEL

The writer notes, as a result of an extensive literature survey [Ref. 1 to 24], that the QFD concept is consistently reported to be a systematic, structured and an effective planning and guidance tool which results in a well designed product which usually meets or exceeds customer requirements. According to Cohen [Ref. 1], probably the most widely used QFD model in the United States is a four-level model known as the Clausing model or the American Supplier Institute (ASI) model. However, it must be noted that in QFD, there is no limit to the number of matrix levels. The four-level QFD model suggested by Clausing consists of performance parameters, parts deployment, manufacturing process and controls. The four-level QFD model is shown in Figure 1.

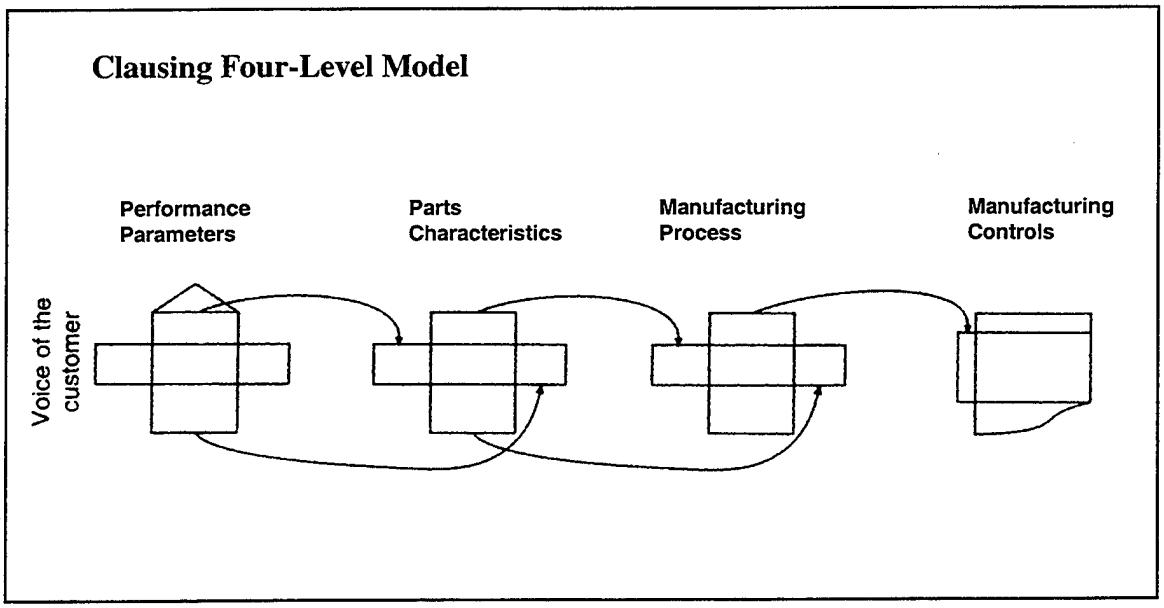

Figure 1. Clausing Four-Level QFD Model. [After Ref. 1].

Interestingly, the writer's literature survey on QFD showed that most organizations do not utilize more than the first QFD matrix, commonly termed a House of Quality. The writer's opinion is that it is likely that organizations are reluctant to share their design thought processes openly as these are sometimes regarded as proprietary knowledge and therefore zealously guarded.

The writer's research goal is to show that QFD can be used effectively during the conceptual design phase of an aircraft. The outcome of the thesis is a four-level QFD conceptual design template for a low speed High Altitude Long Endurance (HALE) Uninhabited Aerial Vehicle (UAV). The Global Hawk design, being a HALE UAV, will be used as a baseline in developing a HALE UAV QFD template. It is expected that the HALE UAV QFD template discussed herein will provide aircraft design teams with a useful tool for the conceptual design of aircraft in general and UAVs in particular.

C. APPLICATION OF QFD TO HALE UAV

To develop the four-level QFD matrix model for the conceptual design of aircraft, the writer choose to focus on UAV mission requirements similar to those of the Global

Hawk. The reason for selecting a UAV for this four-level QFD model is that UAVs represent a potentially large future growth in aircraft production quantities due to potential cost savings and increasing operations requirements. Another reason is that UAVs are free from constraints imposed by aircrew on board.

D. MISSION AND CHARACTERISTICS OF THE GLOBAL HAWK

A brief background of the Global Hawk concept is presented here. Current developmental work is being carried out in a bold attempt to replace expensive manned reconnaissance aircraft, such as the U2 and the SR71, with the Global Hawk (see Figure 2), an autonomous, high altitude long-endurance uninhabited aircraft [Ref. 6].

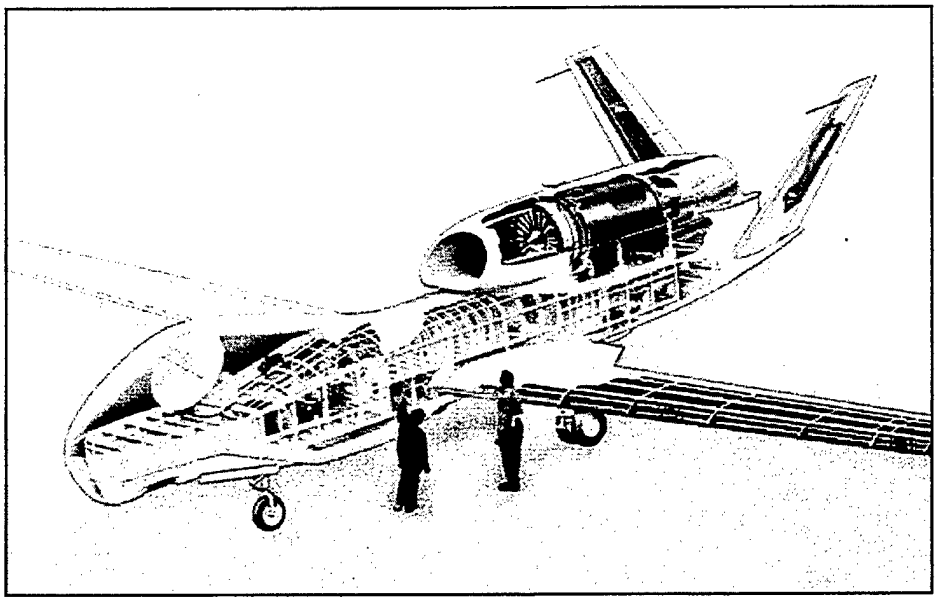

Figure 2. Global Hawk. [From Ref. 6].

The Global Hawk UAV is a multi-purpose, HALE, broad area theater reconnaissance and surveillance system. The Global Hawk is designed to provide 24-hour continuous coverage of interest at long range from the base of operation. The Global Hawk is to be optimized for supporting low-to-moderate threat, long endurance surveillance missions in which range, endurance and time on station are paramount. The survivability of the Global Hawk system is enhanced by its ability to cruise at an altitude

of 65,000 feet, increasing the difficulty for hostile weapon systems' engagement. [Ref. 6].

For this thesis, the HALE UAV desired characteristics are adapted from the Global Hawk descriptions presented in the UAV Annual Report FY 1997 [Ref. 7] and summarized in Table 1 below.

HAE UAV Characteristics		
Altitude	Maximum (km, ft)	19.8 km; 65,000 ft
	Operating (km, ft)	15.2 – 19.8 km; 50,000 – 65,000 ft
Endurance	Max (hrs)	40 hrs, 24 hrs at 5,556 km; 3,000 nm
Radius of Action	(km, nm)	5556 km; 3,000 nm
Speed	Maximum	750 km/h ; 466 mph
	Cruise	600 km/h ; 373 mph
Climb Rate	Maximum	1,036 m/min; 3400 fpm
Deployment		Self Deployable
Propulsion	Engine	One Turbofan /
	Fuel	Heavy Fuel (JP-8)
Weight	Payload	889 kg; 1960 lb
Launch and Recovery	Runway	1,524 m / 5,000 ft
Load Factor		3 gs (max)
Turn Rate		10 deg/s
TAT		1 hour maximum
Unit Cost		Inexpensive

Table 1. UAV Design Characteristics. [After Ref. 7].

II. THE QFD PROCESS

To remain competitive and to sustain continued success in today's environment, a company must ensure that their products not only meet, but exceed customers expectations in terms of quality, cost and desired performance. From the company's perspective, the product is to be built cost-effectively, with optimized resources and within schedule. This means a careful and acceptable balance of design trade-offs is required by prioritizing what is most important to the customer against the array of design characteristics. How can a design team assure that a set of balanced trade-offs will ultimately achieve a winning product? One effective and proven method of translating the customer's voice to the actual product is by applying Quality Functional Deployment (QFD) as a conceptual approach for product system integration.

A. WHAT IS QFD?

To understand QFD, one needs to appreciate its origins. QFD as an approach to design was a concept first introduced in Japan in 1966 by Dr. Yoji Akao [Ref. 4]. He was then the Chairman of the QFD Research Committee of the Japanese Society for Quality Control. QFD is derived from Japanese characters, "hin shitsu" (Qualities); "ki no" (Function) and "ten kai" (Development, Deployment or Diffusion) [Ref. 1]. The "House of Quality" is the basic operational concept of the management approach known as Quality Functional Deployment (QFD). In 1983, Akao introduced QFD into United States [Ref. 1].

Akao [Ref. 4] emphasized that with each new product, the logical system integration approach must begin from the conceptualization phase while looking downstream towards the qualities that customers will demand in the finished product [Ref. 4]. The customer's voice must be systematically integrated into the design process. QFD is a means to assure that a design is essentially stable before production begins or before the prototype is built. QFD, when applied correctly, is the true leverage to a company being competitive. For example, Figure 3 illustrates the significance in terms

of cost savings (and thus improving cost effectiveness and competitiveness) when changes are made early in the conceptual design stage.

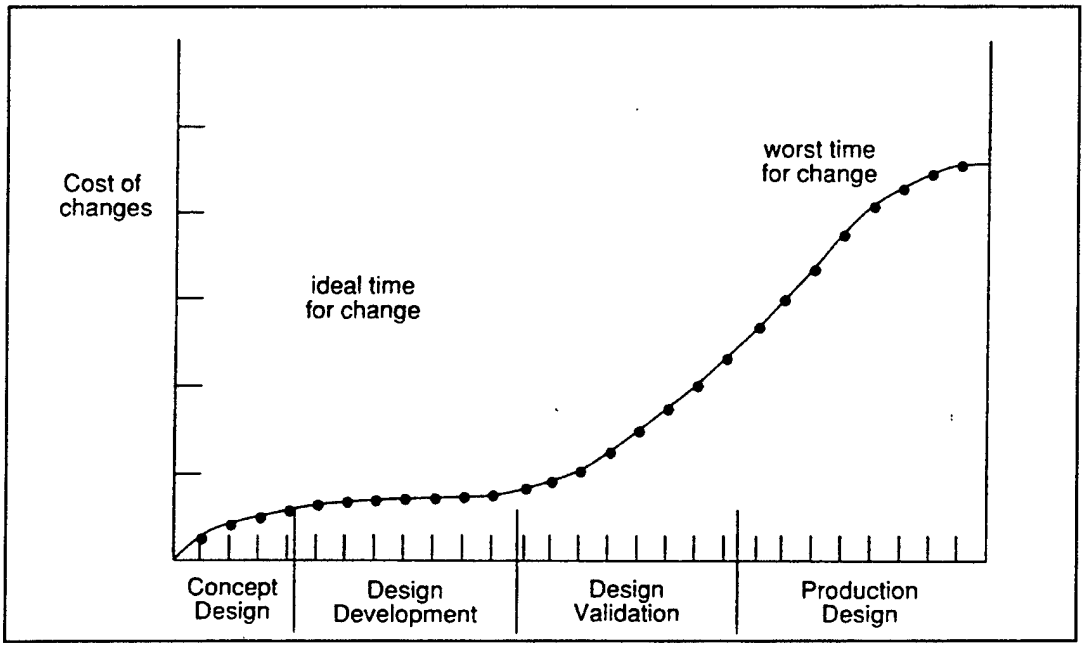

Figure 3. Cost of Changes During Design. [From Ref. 2].

The benefits of QFD are summarized succinctly by Bossert [Ref. 2] and listed here.

- **Customer Driven Attributes**
  - Creates focus on customer requirements.
  - Uses competitive information effectively.
  - Prioritizes resources.
  - Identifies items that can be acted upon.
  - Structures resident experience / information.
- **Reduces Implementation Time**
  - Decreases midstream design change.
  - Limits post-introduction problems.
  - Avoids future unwanted redundancies.
  - Identifies future application opportunities.

- **Promotes Teamwork**
  - Consensus based.
  - Creates communications at design interfaces.
  - Identifies actions at design interfaces.
  - Creates global view out of details.

- **Provides Documentation**
  - Documents the rationale for design.
  - Is easy to assimilate.
  - Adds structure to information.
  - Adapts to changes, a living document.
  - Provides a framework for sensitivity analysis.

B. QFD USE TODAY?

The writer's literature survey on QFD revealed wide and varied applications. Examples noted include aircraft inlet performance, space propulsion system, the conceptual design of a high speed civil transport, automobile design and software. There are even typical applications that do not fit the model of product development. For example, non-product examples quoted by Cohen are course designs, corporate group strategies, telephone service and response service. These far reaching applications underline the flexibility of the QFD tool. [Ref. 1].

C. DECISION TOOLS IN QFD

QFD utilizes certain problem-solving and planning devices initially drawn from a set of tools called the "Seven Management Planning Tools" [Ref. 1]. These devices are essentially decision-making tools based on the Total Quality Management (TQM) concepts and only four planning tools are discussed here. However, only the Matrix Diagram and the Prioritization Diagram devices are used in this thesis.

1. Affinity Diagram

The Affinity Diagram organizes qualitative information and orders the ideas in a hierarchical fashion, working from lower order ideas to higher ones. The relationships of the ideas are based on the ***intuition*** of the design team. This tool is used to collate and organize customer attributes, in a bottom-up approach, to establish main categories of information. For example, take car controls, i.e. turning on the windscreen wipers, figuring out how to set the car clock, seat adjustments, etc. These can be summed up under the higher idea of "intuitive car adjustment controls". [Ref. 1].

2. Tree Diagram

The Tree Diagram is also a hierarchy of ideas. However, unlike the Affinity Diagram the Tree Diagram process flow is built from top down, and is used to complete and to refine the Affinity Diagram. The reverse of the Affinity diagram is applied in the Tree Diagram and is used as a means of cross-checking the hierarchy of ideas. [Ref. 1].

3. Matrix Diagram

The Matrix Diagram maps the relationships between the Whats and the Hows list of ideas or concepts. The matrix is divided into horizontal (Whats) and vertical (Hows) columns. There may be several Hows to achieve each What. For example, a reliable mouse trap (What) may be achieved through "Hows" such as a "High Mean Time between Failures" (MTBF), "time-to-kill" and "dead-mouse-kill / mouse-trap-activation ratio". The Matrix Diagram is also a means to weigh the relative importance of each relationship by allocating numerical values to each What and How. For example, for a reliable mouse trap, the MTBF may be prioritized as a strong positive relationship while the time-to-kill may be a moderate positive relationship. Each level of relationship is accorded different numerical values. [Ref. 1].

4. Prioritization Diagram

Based on the computations in the Matrix Diagram, the ideas are prioritized for further deployment into QFD sub-matrices and treated in the same manner. For example,

the bottom rows of the QFD matrix scores will be a means to prioritize the Hows into Whats of the subsequent QFD matrix.

D. HOUSE OF QUALITY

For this thesis, the QFD process begins with the HALE UAV performance parameter deployment as the first House of Quality. The first matrix (Performance Parameters) Hows are then deployed as Whats in the next matrix (Part Characteristics). This process of deploying the Hows as Whats in subsequent matrices is continued for as many matrices as required. For the purpose of this thesis, the QFD will be limited to four levels. The general House of Quality template for all four deployments is shown in Figure 4.

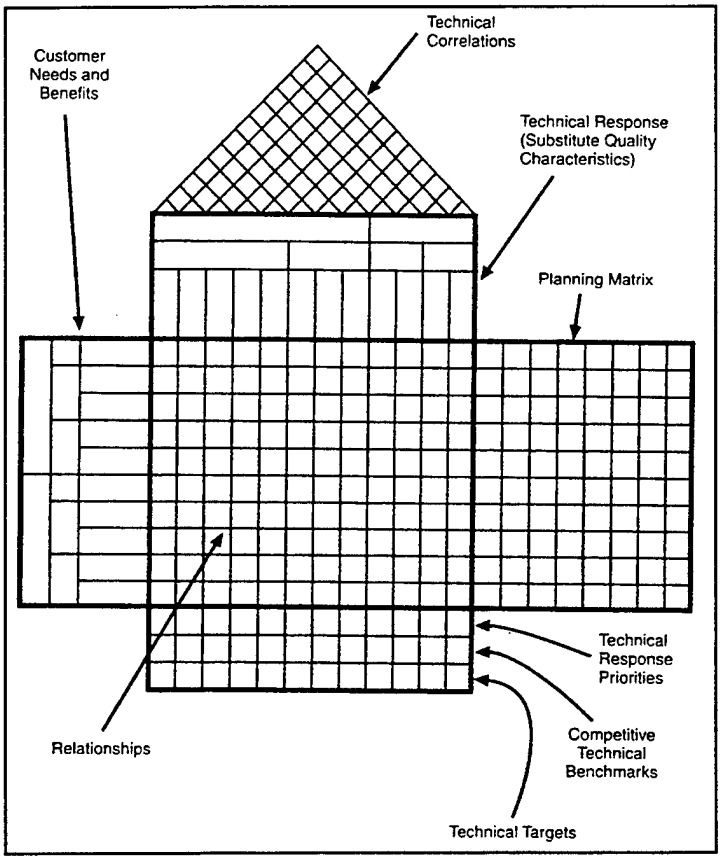

Figure 4. House of Quality. [From Ref. 1].

Typically, the House of Quality, shown in Figure 4, would map out the relationships between the customer voice (wants and needs) and the engineering voice (technical response). Figure 5 shows each of these sections (A to F). The sections shown in Figure 5 are a structured, systematic description of a product or process development team's understanding with regards to the conceptualization of the final product. The lettering sequence, suggested by Cohen, is one logical sequence of developing each matrix and is the one used in this thesis [Ref. 1]. Other sequences might be developed.

Section A contains a structured list of customer wants and needs, i.e., the Request for Proposal (RFP) requirements for the a HALE UAV. Section B may consist of quantitative market data, strategic goal setting by design team or computations for rank ordering the customer attributes.

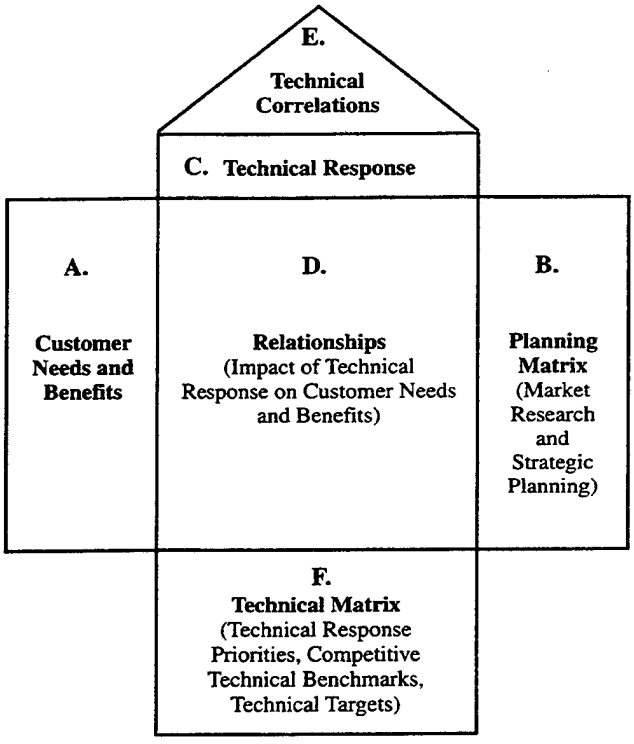

Figure 5. Logical Sequence of Developing the QFD Matrix. [From Ref. 1].

Section C is the technical response by the design team to the customer attributes. This is in the technical design language describing the product performance parameters. Section D is the design team's evaluations of the strength of the relationship between each element of their technical response and each customer attribute. Section E is a matrix showing the design team's judgments of the implementation interrelationships between elements of the technical response. This is also often termed the roof of the house and in essence maps possible trade-off considerations. Section F prioritizes the technical responses (based on weightings, developed earlier by the design team in Section D, given to relative importance of customer attributes, benchmarking competition's current technical performance and the team's technical targets. The writer's research effort is limited to parts A, C, D, E and, to some degree, F. Market research, benchmarking and technical targets were not considered to be within the scope of the thesis.

This page is intentionally left blank.

III. QFD MATRIX 1: DEPLOYING CUSTOMER ATTRIBUTES TO PERFORMANCE PARAMETERS

This chapter discusses the QFD process for deploying the customer's voice against HALE UAV system performance parameters. Design features will also be identified for trade studies.

A. GATHERING THE VOICE OF THE CUSTOMER

Obtaining the customer voice is obviously a crucial step in the formulation of the QFD process. Since the customer voice decides the final configuration, it is absolutely critical for the design team to understand and correctly interpret the needs and wants of the customer. The customer attributes are deliberated and are typically provided in the RFP (shown earlier at Table 1 in the case of this thesis).

B. UAV PERFORMANCE PARAMETERS

To develop QFD Matrix 1, the writer has translated the customer attributes (Whats) into performance parameters (Hows). The key consideration when establishing performance parameters is that they be measurable and able to be translated to manufacturing requirements. To apply the QFD model to the HALE UAV conceptual design, the following information and data are drawn from available Global Hawk literature to form preliminary design information. This will facilitate the deployment of customer attributes to performance parameters. For example, the Global Hawk aspect ratio, aircraft dimensions, performance requirements are used to calculate the zero-lift drag, endurance and range of the conceptual HALE UAV discussed in this thesis. These calculations will be discussed in more detail in the Rough Order of Magnitude analysis (shown below) to determine the relationship in terms of numerical impact of each performance parameter with the RFP system requirements.

1. Major Dimensions

The Global Hawk wing span is 116 ft. The wing area is 540 sq. ft. The length of the fuselage is 44.4 ft and maximum diameter is 4.4 ft. [Ref. 7].

2. Gross Weight

The Global Hawk gross weight (maximum take-off) is 25,600 lb. The fuel weight is 14,700 lb. Therefore the aircraft weight without fuel is approximately 10,900 lb. [Ref. 7].

3. Zero-Lift Drag Coefficient, $C_{D,0}$

The zero-lift drag coefficient is based on the USAF Stability and Control Datcom method. A MATLAB® program (shown in Appendix A) which performs this calculation approximated the Global Hawk HALE UAV $C_{D,0}$ at 0.0161 (40,000 ft altitude). This $C_{D,0}$ of 0.0161 value compares favorably with 0.0197 at 65,000 ft and 0.0137 at sea level. As a check, this HALE UAV $C_{D,0}$ of 0.0161 compared well with the $C_{D,0}$ (0.015) of a similar sized long endurance and high altitude UAV design by a Mississippi State University's student design team submission for the AIAA (1993/94) competition.

4. Wing Loading (W/S)

A MATLAB program was also written to determine the Constraint Diagram shown in Appendix B. The constraint diagram is discussed in detail in paragraph E of Chapter III. The optimum wing loading associated with the constraint diagram is 40 $\frac{lb}{ft^2}$. The This compares well with the Global Hawk at approximately (25,600 lb, gross weight) / (540 sq. ft, wing area), i.e. at 47 $\frac{lb}{ft^2}$.

5. Airfoil

The variation of maximum lift coefficient with thickness ratio at Reynolds Number 1 x 10^6 is provided by Abbott and von Doenhoff [Ref. 25] . According to Figure 6, for a thickness ratio of 16%, the NACA 66-series of 0.4 design lift coefficient offers a good combination of high t/c and $C_{l_{max}}$ of 1.60 (section value). With split flaps,

the $C_{l,\max}$ (section value) is increased to 2.55. These NACA 66 (see Figure 6) data will be used as initial values for analyzing the impacts of the performance parameters listed in the QFD Matrix.

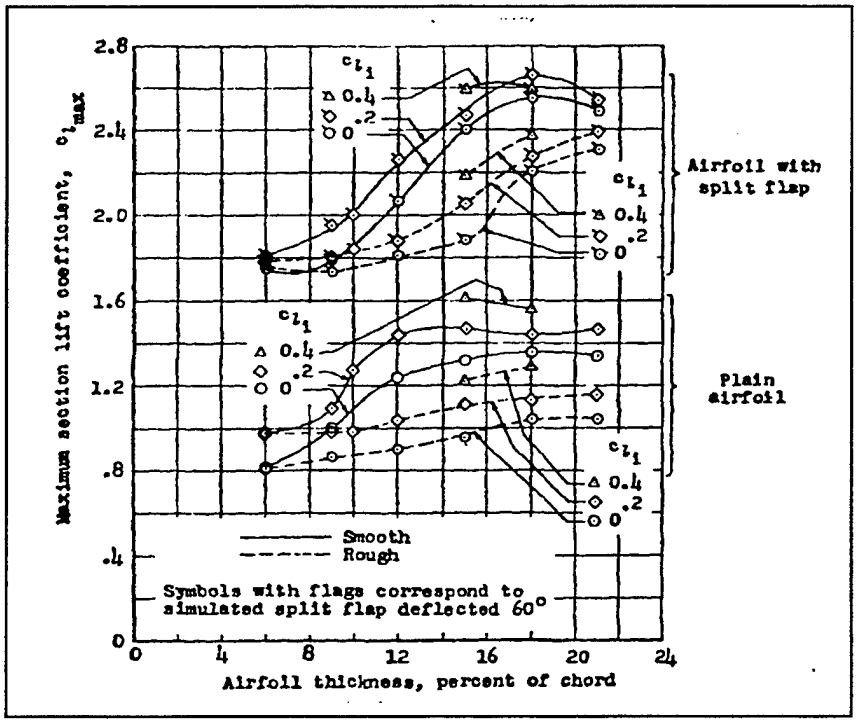

Figure 6. NACA 66-Series. [From Ref. 25].

Figure 6 shows the $C_{l,\max}$ (section value) versus the airfoil thickness for the airfoil and with attached split flaps. There are also different lines to represent the smooth and the rough surfaces. In general, Figure 6 shows that the $C_{l,\max}$ (section value) increases with airfoil thickness (expressed as a percent of chord).

6. Aspect Ratio (AR)

As suggested by Equation (3.1), for a constant wing loading, the HALE UAV would require a relatively higher $C_{L,\max}$ at higher altitudes that at sea level. This is due to the lower densities at higher altitudes.

$$C_{L(\max)} = \frac{W}{0.5\rho V_{stall}{}^2 S} \tag{3.1}$$

The consequence of a high C_L is a high induced drag value. To reduce this induced drag, the high altitude UAV would need a large aspect ratio. For a first estimation, the AR is selected to be 25 (similar to the Global Hawk). The Oswald efficiency is estimated at 0.91.

7. Drag Polar

The HAEL UAV drag polar can be written as

$$C_D = C_{D,0} + \frac{C_L^{\,2}}{\pi e AR} \tag{3.2}$$

Assuming a value of e = 0.91, Equation (3.2) is evaluated as

$$= 0.0161 + \frac{1.60^2}{\pi * 0.91 * 25} = 0.052$$

8. Jet Aircraft Endurance

According to Anderson [Ref. 26], for maximum endurance for a jet aircraft, we want minimum thrust-specific fuel consumption, maximum fuel weight and flight at maximum L/D or $\left(\frac{C_L}{C_D}\right)_{\max}$. The jet aircraft endurance equation from Anderson [Ref. 26] is as follows:

$$E = \frac{1}{C_t}\frac{C_L}{C_D}\ln\frac{W_O}{W_1} \tag{3.3}$$

For maximum aerodynamic efficiency [Ref. 26], we consider:

$$\left(\frac{C_L}{C_D}\right)_{\max} = \frac{\left(C_{D,0}\pi e AR\right)^{1/2}}{2C_{D,0}} \tag{3.4}$$

$$\left(\frac{C_L}{C_D}\right)_{\max} = \frac{\left(0.0161\times\pi\times 0.91\times 25\right)^{1/2}}{2\times 0.0161} = 33.31$$

9. Jet Aircraft Range

According to Anderson [Ref. 26], for maximum range for a jet aircraft, we want minimum thrust-specific fuel consumption, maximum fuel weight, flight at $\left(\frac{C_L^{1/2}}{C_D}\right)_{\max}$ and flight at high altitudes. Anderson [Ref. 26] provides the range equation for the jet aircraft as follows:

$$R = 2\frac{\sqrt{2}}{\sqrt{\rho_\infty S}}\frac{1}{C_t}\frac{C_L^{1/2}}{C_D}(W_O^{1/2} - W_1^{1/2}) \tag{3.5}$$

To maximize jet aircraft range [Ref. 26], we consider:

$$\left(\frac{C_L^{1/2}}{C_D}\right)_{\max} = \frac{(1/3 * C_{D,0}\pi eAR)^{1/4}}{4/3 * C_{D,0}} \tag{3.6}$$

$$\left(\frac{C_L^{1/2}}{C_D}\right)_{\max} = \frac{(1/3 * 0.0161 * \pi * 0.91 * 25)^{1/4}}{4/3 * 0.0161} = 36.66$$

10. Velocities, V

The HALE UAV V_{max} is 466 mph or 683.5 feet per second (fps). The cruise velocity is 373 mph or 546.78 feet per second (fps). These velocities correspond approximately to the Global Hawk velocities.

11. UAV Thrust

The HALE UAV propulsion thrust is evaluated from the Constraint Diagram (see Figure 7). The optimum T/W_{to} is 0.33. Therefore, an initial estimate of the thrust is 0.33 * 25,600 lb = 8,448 lb. This is close to the Global Hawk required thrust of 7,050 lb.

12. TSFC, Ct

Nicolai [Ref. 30] provided a good guide on the range of turbofan TSFC at 0.3 to 1.0 lb fuel / lbf thrust – hour. For this HALE UAV design, the turbofan propulsion TSFC is estimated at 0.60 lb fuel / lbf thrust – hour.

C. ROUGH-ORDER-OF-MAGNITUDE (ROM) ANALYSIS FOR HALE UAV

With the preliminary HALE UAV performance data given above, the next step in QFD Matrix 1 is to select and examine the performance parameters in relation with the operational requirements (customer attributes). The selected categories are aircraft performance, stability, engine performance, structural stiffness and life cycle cost considerations. Using an order-of-magnitude comparison, the performance parameters (Hows) are examined based on their impact on the customer attributes (Whats). Interestingly, the writer noted that the idea of comparing the impact of such parameters is also used by Hale [Ref. 27]. Hale utilizes Figures of Merit for Selection and Design.

The aircraft performance and stability and control equations used for the ROM analysis are taken from Anderson [Ref. 26] and Hale [Ref. 27] and summarized in Table 2. The results in Table 2 are then translated into the QFD Matrix 1. Examples of the ROM analysis to produce Table 2 are shown in Appendix C. In the ROM analysis, the performance parameters are computed individually, while keeping all other parameters constant to determine the order of magnitude effect of each performance parameter on each of the customer attributes.

An explanation of Table 2 is necessary here. Take for example the gross HALE UAV weight (W_o) shown in Table 2. The HALE UAV gross weight should be low to maximize jet endurance. Therefore the down ($\downarrow$) arrow implies the design direction to reduce the gross weight as best as possible. With the first weight estimation of 25,600 lbs, the $\ln\frac{W_o}{W_1}$ component of the endurance Equation (3.3) is equal to 0.85 (the

calculation is shown in Appendix C). This provides a rough order of magnitude of the weight component in having an impact of reducing the endurance by 0.85. The value of 0.85 would be translated as a negative relationship between weight and endurance. This is counter-intuitive to the ($\downarrow$) arrow of the weight (implying a weight reduction) which should increase the UAV endurance. The writer would like to reiterate that the reason for this "counter-intuitive" logic is that the matrix relationships are derived from engineering equations (examples of such calculations are shown in Appendix C).

For another example, the HALE UAV AR is desired to be high ($\uparrow$) as shown in Table 2. The ROM analysis shows that the chosen AR of 25 has an order of magnitude impact of increasing the endurance by an order of 5, range by 2.24, cruise altitude by 5, load factor by 5, turn rate by 5 and reducing the runway length by a factor of 5.

For a third example, consider L/D in Table 2. Similarly, the L/D (which the up-arrow $\uparrow$ means we want a highest possible aerodynamic efficiency) has a 33.31 order of magnitude impact on increasing the HALE UAV endurance. These ROM values in Table 2 are compared with each other and translated into the QFD Matrix 1 into one of four levels, i.e. strong positive, positive, strong negative and negative.

To ensure that these performance parameters are realistic in the development of the HALE UAV design template, it is important to validate these numbers where possible. For example, the endurance of the subject HALE UAV is compared with the Global Hawk. The maximum HALE UAV endurance is computed in Appendix C to be 47.4 hours which is reasonably close to the Global Hawk's published value endurance of 40 hours [Ref. 6].

Performance Parameters	$W_o \downarrow$	$\frac{W}{S} \downarrow$	$\frac{L}{D} \uparrow$	$C_{L_{max}} \uparrow$	$C_{D,0} \downarrow$	AR ↑	T/W ↓	$C_t \downarrow$
Endurance ↑	0.85		33.31	1.60	7.88	5		1.67
Range ↑	6.25 E(-3)	6.32		1.26	22.12	2.24		1.67
Cruise Alt. ↑	3.9 E(-5)				7.88	5		
Max Speed ↑		6.32			7.88		0.57	
Climb Rate ↑	6.25 E (-3)	6.32			7.88		0.19	
Runway ↓	25.6 E (3)	47.4		0.63		5	3.03	
Load Factor ↑		0.02		1.60	7.88	5	0.33	
Turn Rate ↑		0.16				5	0.57	
Note: Impact of parameters are computed while keeping the rest of the parameters constant.								

Table 2. Rough Order of Magnitude (ROM) Analysis.

The ROM analysis is then translated into the QFD Matrix 1 scores. The translation criteria adopted is show in Table 3. Take for example, reducing $C_{D,0}$ would have an impact of a reduction factor of 22.12 on range (shown in Table 2) would be translated into the QFD Matrix 1 as a strong positive relationship between range and $C_{D,0}$.

ROM Analysis (Magnitude)	**QFD Matrix Relationship Score**
≤ 0.1	Strong Negative
≤ 1	Negative
≥ 1	Positive
≥ 10	Strong Positive

Table 3. ROM Scoring Criteria.

D. HUERISTIC ESTIMATES (ROM)

The writer experienced difficulties in obtaining explicit engineering equations to determine the ROM impact of HALE UAV payload, self deployment, turnaround time and availability. In this case, these performance parameter relationships with the customer requirements are determined based on deliberations with faculty members of Aeronautical Engineering [Ref. 29] and then recorded in QFD Matrix 1.

1. Stability and Control

The stability and control equations were reviewed in Anderson [Ref.26] and shown in Equations (3.7) and (3.8). The necessary criteria for longitudinal balance and static stability are that $C_{M,0}$ must be positive and that $\frac{\partial C_{M,cg}}{\partial \alpha_a}$ must be negative. [Ref.26].

$$C_{M,0} = C_{M,ac_{wb}} + V_H a_t (i_t + \varepsilon_0); \text{ and} \tag{3.7}$$

$$\frac{\partial C_{M,cg}}{\partial \alpha_a} = a\left[h - h_{ac_{wb}} - V_H \frac{a_t}{a}\left(1 - \frac{\partial \varepsilon}{\partial \alpha}\right)\right] \tag{3.8}$$

The stability performance parameter has a positive relationship with endurance, range and cruise altitude. For example, if the aircraft is not properly trimmed, there would be unnecessary losses due to excessive pitching moments. Also, excessive trim drag can, for example, reduce range and endurance. Due to its impact on center of gravity location, payload has a positive relationship with longitudinal stability. A properly located payload would minimize the HALE UAV center of gravity shift.

2. Payload

A maximum payload would be positively impacted (more weight means more lift) by a high aerodynamic efficiency, coefficient of lift and high material specific strength. A high payload would mean more avionics, and this can be expected to correspond (correlate positively) to increase in maintainability and a decrease in MTBF. More avionics parts would likely result in higher failure rate (decrease in MTBF). However,

redundant avionics parts may fail without affecting mission success, i.e. MTB Critical Failures goes up. A low wing loading will mean a larger wing area (for a given weight) and thus would allow an incremental increase in payload without changing the wing loading significantly. Conversely, the maximum payload value can be expected to increase the overall UAV weight and thereby negatively affect a desired low gross UAV weight value.

3. Self Deployment

Self deployment requires that the HALE UAV be able to take-off from a runway length of 5000 feet without any assisted boost, e.g. catapult to shorten its take off distance. The runway length requirement was obtained from the Global Hawk literature [Ref. 6]. Self deployment is considered to be a positively influenced by a high aerodynamic efficiency, high coefficient of lift, a high AR, a low engine thrust-to-weight ratio and negatively impacted by the desired low aircraft take-off weight.

4. Turnaround Time (TAT)

The TAT is defined as the time to required to service the HALE UAV upon landing for preparation for the next flight. A low TAT would be expected to have a direct correlation with low aircraft gross weight and low engine thrust-to-weight ratio. For example, keeping other variables constant a lower weight UAV would imply a smaller aircraft and therefore less time to prepare the UAV for the next flight.

5. Availability

Higher aircraft availability would suggest higher Mean Time Between Failure (MTBF) and lower Mean Time To Repair (MTTR) values and likely a higher life cycle cost [Ref. 40].

$$\text{Aircraft Availability, } A_O = \frac{MTBF}{MTBF + MTTR} \tag{3.9}$$

6. Low Cost

Nicolai [Ref. 30] shows how an initial estimate of the LCC cost can be obtained based on limited acquisition and performance parameters. However, only the airframe engineering hours is used in this thesis to indicate the relationship between aircraft performance and cost.

$$E = 0.0396A^{0.791}S^{1.526}Q^{0.183} \tag{3.10}$$

where A = Aeronautical Manufacturers Planning Report (AMPR) weight.

AMPR weight is defined as the empty aircraft weight less wheels, brakes, tires, tubes, engines, starter, cooling fluid, rubber or nylon fuel cells, instruments, batteries and electrical supply, electronics avionics equipment, armament and fire control systems, air conditioning systems, auxiliary power system and trapped fuel and oil. The preliminary estimate is approximately 12,800 lbf (as a first estimate, taking 50% of the Global Hawk gross weight is 25,600 lbf);

S = maximum speed (knots) at best altitude (345 knots); and

Q = number of aircraft to be manufactured (assumed 1000).

Therefore,

$A^{0.791}$ = 1773.08 (low weight has a strong positive relationship with low cost)

It is also reasonable to assume that the initial cost would also decrease with a lower engine T/W ratio (it is likely that a smaller engine would be less expensive), low MTTR and high MTBF. It is noted that the low MTTR and high MTBF factors would hold for small deviations around the design points as they are not necessarily linear with cost. Conversely, it seems reasonable to assume the cost would increase with stronger and more advanced materials.

E. CONSTRAINT DIAGRAM ANALYSIS

Thrust-to-weight (T_{SL}/W_{TO}) ratio and the wing loading are two of the most important parameters affecting aircraft performance. Hence, to complete the QFD Matrix

1 analysis, it is important to consider how a constraint diagram analysis will impact aircraft performance parameters. The master equation, shown as Equation (3.11), for the constraint diagram is based on the 1st Law (Conservation of Energy). [Ref. 28].

$$(T-D)V = W\frac{dh}{dt} + \frac{W}{g_c}\frac{d}{dt}\left(\frac{V^2}{2}\right) \tag{3.11}$$

that is; rate of mechanical energy input = storage rate of potential energy + storage rate of kinetic energy.

Equation (3.8) is further expanded in Mattingly [Ref. 28] to the master equation;

$$\frac{T_{SL}}{W_{TO}} = \frac{\beta}{\alpha}\left\{\frac{qS}{\beta W_{TO}}\left[k\left(\frac{n\beta}{q}\frac{W_{TO}}{S}\right)^2 + C_{D,0}\right] + \frac{1}{V}\frac{d}{dt}\left(h + \frac{V^2}{2g}\right)\right\} \tag{3.12}$$

which includes installed thrust lapse and instantaneous weight lapse equations. The thrust lapse and weight lapse equations are given by:

$$T = \alpha T_{SL} \text{ ; and} \tag{3.13}$$

$$W = \beta W_{TO} \text{ , respectively.} \tag{3.14}$$

The UAV mission profile consist of ten segments as follows:

- Take Off Ground Roll
- Constant Speed Climb
- Constant Altitude / Speed Cruise
- Constant Altitude / Speed Turn
- Maximum Speed
- Horizontal Acceleration
- Instantaneous Turn
- Service Ceiling
- Sustained Turn
- Landing

Equation (3.12) is specialized for each of these ten mission segments, e.g. dh/dt = 0 for constant altitude flight and dV/dt = 0 for constant velocity flight. The 10 mission segments are shown in Figure 7. These 10 mission segments curves were generated by

developing a MATLAB® code written by the writer and given in Appendix B. The AR and the $C_{D,0}$ were kept constant for the constraint diagram shown in Figure 7. The acceleration performance curve in Figure 7 is the decisive constraint in obtaining the optimum T_{SL}/W_{TO} (0.34) and W_{TO}/S (37 psf) parameters for the HALE UAV design template development.

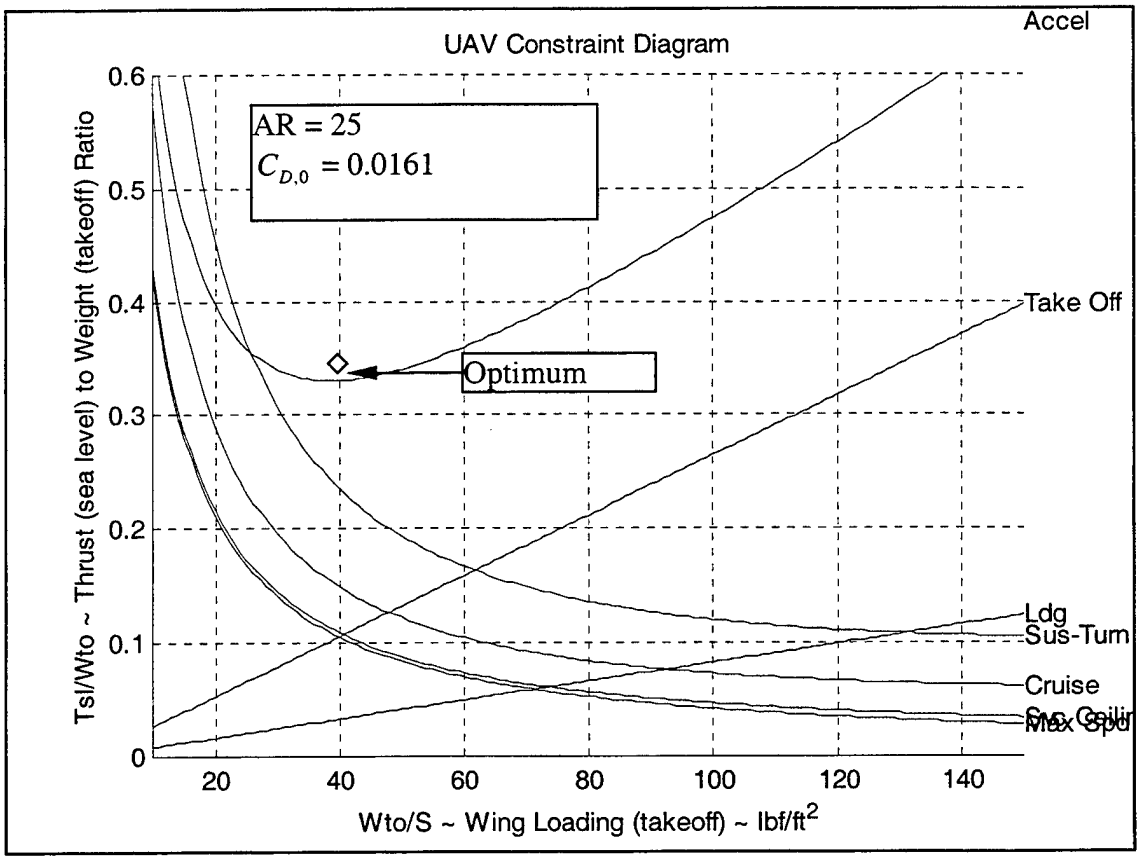

Figure 7. Constraint Diagram.

The question now remains to how can we incorporate the results from the constraint diagram into scores in the QFD Matrix 1. The details of score calculations is detailed in Section C (Table 2) above. In examining the acceleration equation, the writer noted there are two performance parameters, i.e. AR and $C_{D,0}$ that impact the optimum T_{SL}/W_{TO} and W_{TO}/S ratios. These two parameters (AR and $C_{D,0}$) are further varied to

investigate the impact on the constraint plot optimum point. The plan for varying the AR and $C_{D,0}$ is shown in Table 4 and the results plotted in Figure 8.

Performance Parameters	Trial 1: Variation with 120 % AR only	Trial 2: Variation with 80 % $C_{D,0}$ only
Cl = 1.60	Cl = 1.60	Cl = 1.60
AR = 25	AR = 30	AR = 25
$C_{D,0}$ = 0.0161	$C_{D,0}$ = 0.0161	$C_{D,0}$ = 0.01288

Table 4. AR and $C_{D,0}$ Sensitivity Constraint Trials on T_{SL}/W_{TO}.

Another MATLAB® code (see Appendix D) was written to show the impact of the individual performance parameter on the HALE UAV Acceleration curve as shown in Figure 8.

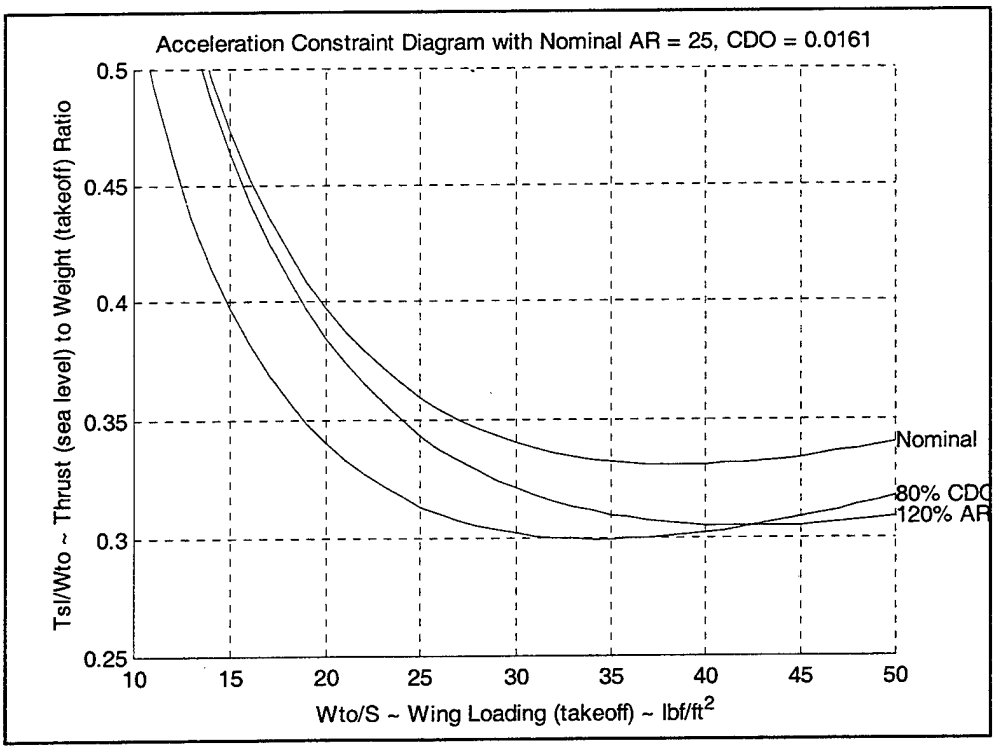

Figure 8. Sustained Turn Constraint Sensitivity Study.

The results of Figure 8 are tabulated in Table 5. The acceleration "trial 1" curve, i.e., with 120% increase in AR has the effect of a reduction of T_{SL}/W_{TO} by 93% and increase the W_{TO}/S by 106%. Trial 2 acceleration curve, i.e. with a 80% reduction of $C_{D,0}$ would result in a reduction of T_{SL}/W_{TO} by 91% and decrease the W_{TO}/S by 87.5%.

	T_{SL}/W_{TO}	W_{TO}/S (psf)
Without variations (Nominal Results)	0.33	40
120 % AR (Trial 1)	0.31 (93 %) ↓	42.5 (106 %) ↑
80 % $C_{D,0}$ (Trial 2)	0.30 (91 %) ↓	35 (87.5 %)↓

Table 5. Results of Impact of AR and $C_{D,0}$ on T_{SL}/W_{TO}.

The impact of AR and $C_{D,0}$, shown in Table 5, on the engine thrust-to-weight ratio and the wing loading are then scored in the roof of QFD Matrix 1.

F. IMPACT OF QFD MATRIX 1

The QFD Matrix 1 is assembled in Figure 9. In the column "Importance" of QFD Matrix 1, Figure 9, the customer attributes are prioritized. For example, the endurance is weighted highest 13 is the most important customer attribute. The row "Relative Importance" in Figure 9 is obtained by multiplying the weighted importance against the individual columns of performance parameters. The relationship symbols used in the QFD matrices and the corresponding scores are assigned as follows:

- ⊙ Strong Positive (+, 2 points)
- O Positive (+, 1 point)
- # Strong Negative (-, 2 points)
- x Negative (-, 1 point)

The relative importance is then translated into weight importance of each performance parameter (Hows) which becomes the Hows weighted importance for the next QFD matrix. For example, the Relative Importance score of negative 100 for gross weight (W_O), is obtained by multiplying the values of the W_O column against the values (weightings) of the Importance column of the customer attributes. This W_O Relative Importance score of negative 100 is compared with the other scores of performance parameters and then the highest absolute scores are prioritized (weighted) highest. In this case, W_O which has a score of absolute 100 is weighted highest at the value of weight of 13.

The arrows in the "direction of improvement" matrix row in Figure 9 documents the direction that the design should work towards. For example, for the HALE UAV, the gross weight should be as low as possible ($\downarrow$), while the L/D ($\uparrow$) should be maximized to achieve the best possible endurance and range.

QFD Matrix 1 shows that to achieve the operational requirements, the design team has to first focus on ensuring that those performance parameters with highest scores (in Relative Importance) are given highest priority in the HALE UAV design. QFD Matrix 1 shows that the four most important performance features that significantly contribute to the customer requirements are low gross aircraft weight, low zero-lift drag, high maximum coefficient of lift and low life cycle cost. QFD Matrix 1 identifies the most important performance parameters (highest scores) and thereby allows the design team to focus on these parameters that are crucial to meeting the customer requirements or operational requirements of the HALE UAV. The design team also needs to perform trade studies where there are conflicting directions of improvement as seen in the QFD Matrix 1 roof. In addition, the design team needs to review the negative relationships in the matrix. For example, the significance of the large negative score of the gross weight component against the customer attributes would be that it may offer an opportunity for breakthrough ideas to effectively enhance the overall conceptual HALE UAV design.

The "roof" of the matrix or the Technical Correlations provide a mechanism where one compares each parameter against another to determine whether or not there are conflicting design requirements or bottlenecks, and therefore show potentially where design conflicts need to be evaluated. The design conflicts are summarized in Table 6. These conflicts must be addressed at the conceptual design stage so as to ensure minimal changes downstream.

Performance Parameters		UAV HALE Design Areas To Be Evaluated
$W_O \downarrow$	$L/D \uparrow$	Now, to achieve $\left(\frac{C_L}{C_D}\right)_{\max} = \frac{\left(C_{D,0}\pi eAR\right)^{1/2}}{2C_{D,0}}$; the design team may select a large Aspect Ratio (holding other variables constant). The larger AR would likely lead to an increase in aircraft gross weight.
$W/S \downarrow$	$L/D \uparrow$	If the W / S is decreased by means of a larger wing area, then the AR is reduced, which may lead to a lower L / D.
$W/S \downarrow$	$C_{D,0} \downarrow$	If the W / S is decreased by increasing wing area, the zero-lift drag will increase due to the dominant factor of friction.
$W/S \downarrow$	$AR \uparrow$	If W/S is reduced by means of increasing wing area, S – then the design team has to note that that AR will be reduced (for b held constant). This is because $AR = b^2/S$.
$C_{L,\max} \uparrow$	$C_{D,0} \downarrow$	Increasing $C_{L,\max}$, say by having a thicker airfoil or requiring flaps down during cruise, would increase $C_{D,0}$. The design team has to be aware that an airfoil offering a higher $C_{L,\max}$ would likely be obtained at the expense of a higher $C_{D,0}$.
$AR \uparrow$	$LCC \downarrow$	A higher aspect ratio will likely incur a higher cost.

Table 6. QFD Matrix 1: HALE UAV Design Areas for Trade Studies.

QFD Performance Parameters Matrix

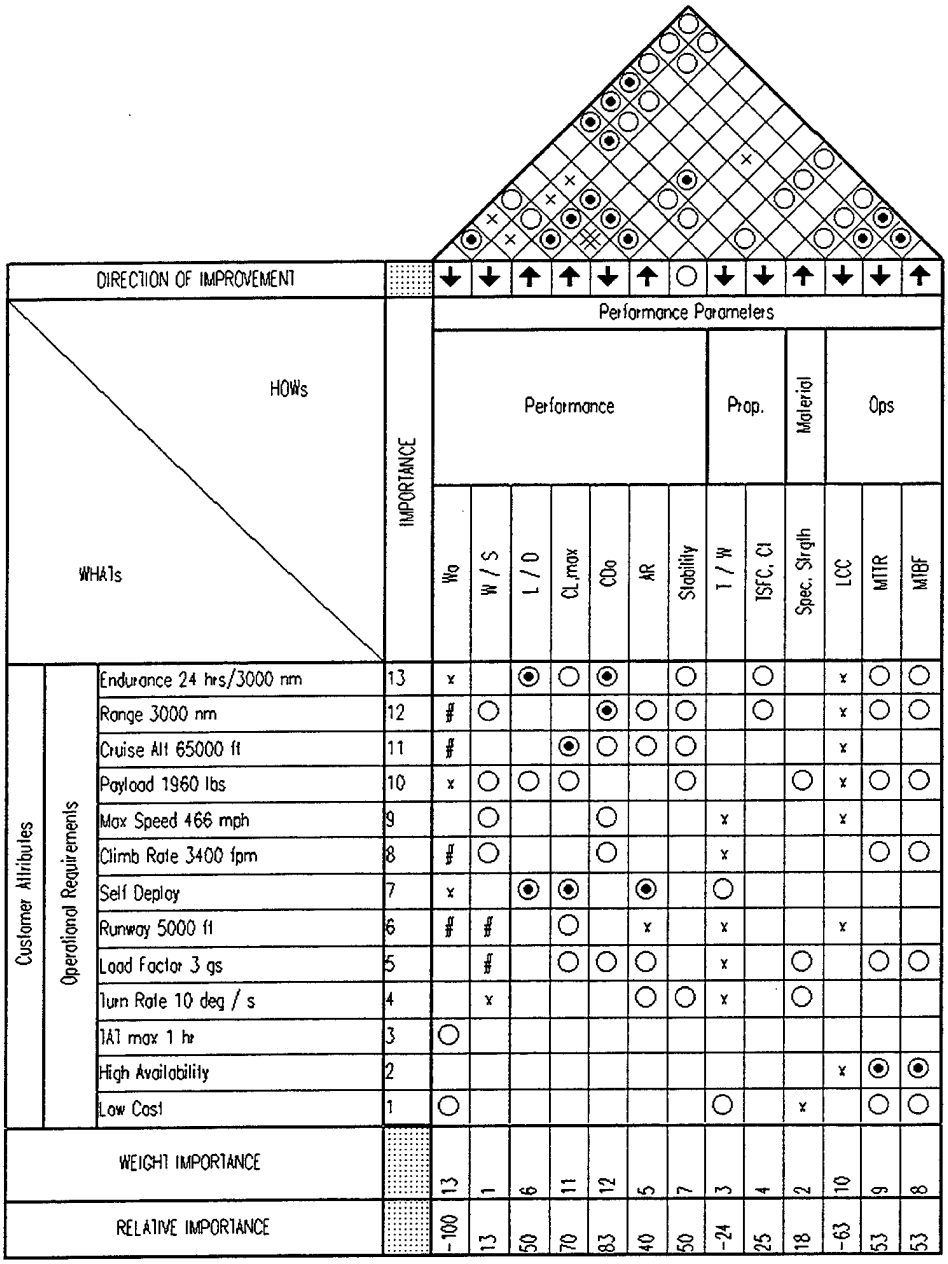

DIRECTION OF IMPROVEMENT			↓	↓	↑	↑	↓	↑	○	↓	↓	↑	↓	↓	↑
WHATs \ HOWs		IMPORTANCE	Performance Parameters												
			Performance							Prop.		Material	Ops		
			Wo	W / S	L / D	CL,max	CDo	AR	Stability	T / W	TSFC, Ct	Spec. Strgth	LCC	MTTR	MTBF
Customer Attributes / Operational Requirements	Endurance 24 hrs/3000 nm	13	x		◉	○	◉		○		○		x	○	○
	Range 3000 nm	12	#	○			◉	○	○		○		x	○	○
	Cruise Alt 65000 ft	11	#			◉	○	○	○				x		
	Payload 1960 lbs	10	x	○	○	○			○			○	x	○	○
	Max Speed 466 mph	9		○			○			x			x		
	Climb Rate 3400 fpm	8	#	○			○			x				○	○
	Self Deploy	7	x		◉	◉		◉		○					
	Runway 5000 ft	6	#	#		○		x		x			x		
	Load Factor 3 gs	5		#		○	○	○		x		○		○	○
	Turn Rate 10 deg / s	4		x				○	○	x		○			
	TAT max 1 hr	3	○												
	High Availability	2											x	◉	◉
	Low Cost	1	○							○		x		○	○
WEIGHT IMPORTANCE			13	1	6	11	12	5	7	3	4	2	10	9	8
RELATIVE IMPORTANCE			-100	13	50	70	83	40	50	-24	25	18	-63	53	53

Figure 9. HALE UAV QFD Matrix 1.

IV. QFD MATRIX 2: DEPLOYING PERFORMANCE PARAMETERS TO PART CHARACTERISTICS

With QFD Matrix 1 completed, the performance parameters requirements may be deployed to the part characteristics in QFD Matrix 2. It is emphasized that the design team frequently reviews completed matrices when new information is added since these changes may influence the other matrices. In QFD Matrix 2, the design team should already have some preliminary design ideas and directions as the part characteristics need to be specific to meet the performance parameters. For example, for a subsonic HALE UAV, the airfoil may require a high thickness to chord ratio to accommodate more fuel and one would also expect a small wing sweep angle for a sail-plane wing design [Ref. 34].

A. PARTS DEPLOYMENT

The following key aircraft parts are deemed important when deploying the performance parameters to part characteristics in the conceptualization stage of the HALE UAV. Unlike QFD Matrix 1, the writer finds that the relationships between the performance parameters and the parts characteristics in QFD Matrix 2 are largely empirical.

1. Airfoil Thickness/Chord (t/c) Ratio

The coefficient of lift increases with an increase with the airfoil t/c ratio. This is noted in Abbott and von Doenhoff [Ref. 25] and Nicolai [Ref. 30]. The relationship between a subsonic aircraft wing and airfoil t/c ratio is as follows [Ref. 30] .

$$W = 0.00428(S_W)^{0.48} \frac{AR(M_O{}^{0.43})}{(100t/c)^{0.76}} \frac{(W_{TO}N)^{0.84}\lambda^{0.14}}{(\cos\Delta_{1/2})^{1.54}} \qquad (4.1)$$

Therefore, for a chosen value of airfoil thickness-to-chord ratio, i.e., 0.16, Equation (4.1) shows that (holding other variables in the equation constant) the wing weight is impacted by a factor of 4. Therefore, it is noted that the effect of a thicker airfoil would result in a decrease in weight. Furthermore, Anderson [Ref. 26] also

mentioned that a thicker airfoil (for low Mach cruise) has the advantage of ease in structural design, lightweight and provides more volume in fuel capacity.

2. Wing Sweep Angle

Nicolai [Ref. 30] provided the relationship between the wing sweep (Λ) and the aspect ratio, AR, i.e.

$$\tan\Lambda_{LE} = \tan\Lambda_{C/4} + \left[(1-\lambda)/AR(1+\lambda)\right] \tag{4.2}$$

$$\text{where } \lambda = \frac{C_t}{C_r} \text{ (taper ratio)} \tag{4.3}$$

For a given taper ratio and a quarter chord sweep angle, Equation (4.2) shows that an decrease in AR would result in a marginal increase in wing sweep angle. For a low speed flight such as the Global Hawk, or any high altitude UAV, it is advantageous to have a high AR. Although wing sweep increases the drag divergence Mach number, it also serves to decrease coefficient of lift. Also as seen in the Equation (4.1), a small decrease in sweep would result in a proportionally small decrease in aircraft weight.

3. Ailerons and Spoilers

Ailerons are "flaps" mounted close to the wing tips for lateral control. The ailerons would serve to increase or decrease the lift for a specific roll input and would thereby add to the wing zero-lift drag. Spoilers are "lift dumpers" which would spoil the lift over the surface immediately behind the spoiler. The deployed spoiler on a HALE UAV has a negative relationship with the zero-lift drag, i.e., $C_{D,0.}$ increases.

4. Trailing Edge (TE) Flaps

To increase lift, the aircraft can increase its angle of attack (AOA) or have a larger camber or both. Trailing edge flaps provide both these features. The following figure from Anderson [Ref. 26] illustrates this empirical relationship.

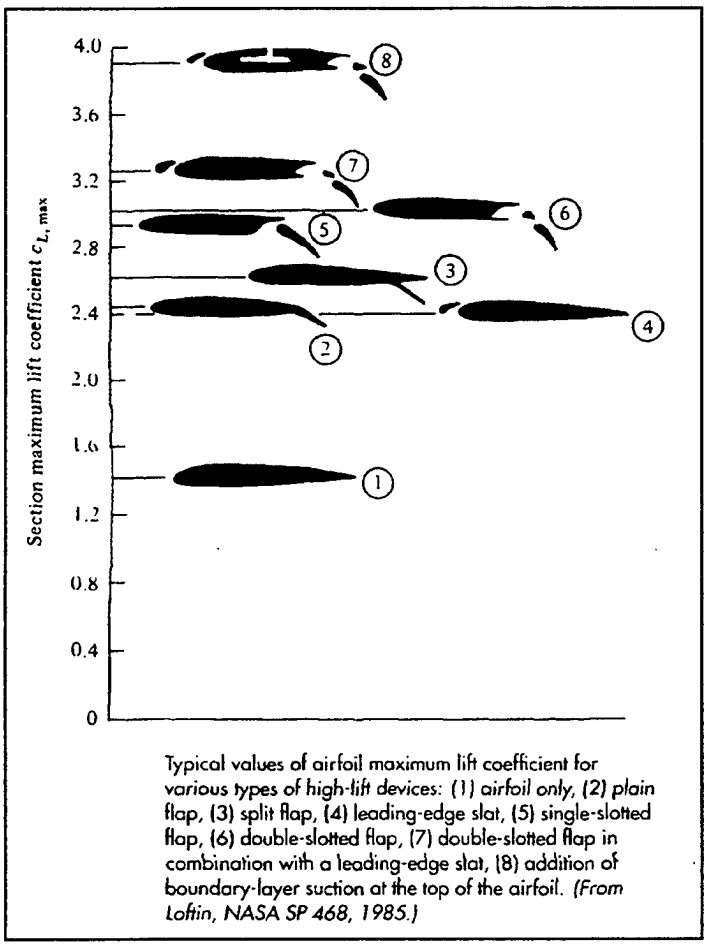

Typical values of airfoil maximum lift coefficient for various types of high-lift devices: (1) airfoil only, (2) plain flap, (3) split flap, (4) leading-edge slat, (5) single-slotted flap, (6) double-slotted flap, (7) double-slotted flap in combination with a leading-edge slat, (8) addition of boundary-layer suction at the top of the airfoil. *(From Loftin, NASA SP 468, 1985.)*

Figure 10. Increase of Lift with TE Flaps. [From Ref. 26].

5. Empennage

It is noted that the Global Hawk has a V-tail and this design is used as a reference to derived the importance of the empennage. Roskam Part III [Ref. 31] stated that a V-tail design would result in a smaller wetted area and less weight compared with a conventional empennage arrangement. The effective function of a tail is to create uplifts or downlifts to generate a moment about the aircraft center of gravity, thereby counteracting the moments generated by the wing. Thus it would be expected that the tail size be related to the wing size.

6. Fuselage Fineness Ratio

The fuselage fineness ratio is defined as the fuselage length divided by the maximum fuselage diameter. Nicolai [Ref. 30] showed a empirical relationship of zero-lift drag versus the inverse of fineness ration, reproduced in Figure 11.

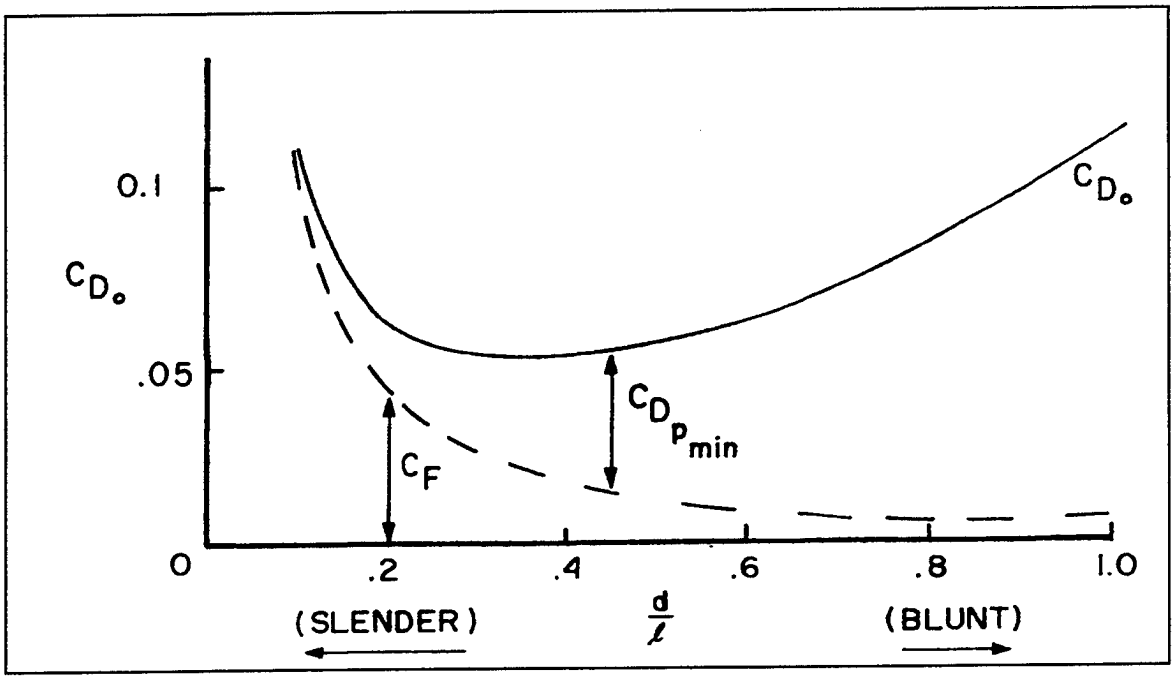

Figure 11. Impact of Fineness Ratio on $C_{D,0}$. [From Ref. 30].

It is seen that the $C_{D,0}$ is predominantly due to viscous separation. The $C_{D,0}$ (min.) is at fuselage diameter / length of approximately 0.33. The subsonic $C_{D,0}$ for a fuselage is a compromise between skin friction drag coefficient and the pressure drag coefficient. The fuselage should be a streamlined shape with tapered ends. A blunt aft fuselage end would cause flow to separate with large increase in $C_{D,0}$ due to after-body flow separation.

7. Number of Engines

It is suggested that as the number of engines is increased one would expect to see a significant increase in life cycle cost, weight, fuel consumption and $C_{D,0}$. These have

the consequence of increased wing loading, and reduced aerodynamic efficiency, i.e. $\left[\frac{L}{D}\right]_{max}$ if the $C_{D,0}$ increases. However, these factors would have to be studied carefully in the light of engine reliability. Given a highly reliable engine, the author would be inclined to select a single engine for reasons mentioned.

8. Engine Type

The thrust of a turbofan engine is a combination of thrust produced by the fan blades and the thrust of the jet from the primary exhaust nozzle. Consequently, the efficiency of the turbofan engine offers better specific fuel consumption than the jet engine. It is noted that the Allison AE 3007 (turbofan) was selected for the Global Hawk. In order to draw the importance of the turbofan engine with regards to the HALE UAV performance, the writer selected the best mileage per pound fuel relationship from Hale [Ref. 27].

$$\text{Best Mileage/lb fuel for Range} = \frac{25}{C_t W}\sqrt{\frac{(W/S)}{\sigma}}\left[\frac{e(AR)}{C_{D,0}{}^{3}}\right]^{1/4} \qquad (4.4)$$

Substituting typical numbers into Equation (4.4), allows one to estimate the effect of the various parameters upon the range (best mileage/lb fuel) of the HALE UAV. The rough order-of-magnitude (ROM) analysis on Equation (4.4) is shown in Table 7. The performance parameter values are obtained from Chapter III. Table 7 suggests that the performance parameter impacts are all positive with a low $C_{D,0}$ having the most significant impact on increasing HALE UAV range. Also, as expected, the higher the HALE UAV weight component, the more adverse is the best mileage per pound fuel.

	C_t	W	W/S	AR	$C_{D,0}$
Performance Parameters Values	1/0.6	1/25,600	$\sqrt{40}$	$25^{1/4}$	$\frac{1}{0.0161^{3/4}}$
ROM Impact on Best Mileage/lb fuel	1.67	3.9 E(-5)	6.32	2.24	22.12

Table 7. Impact of Fuel Consumption on Engineering Characteristics.

9. Inlet Design

Roskam [Ref. 31] stated that the objectives of inlets are to provide the correct amount of airflow to the engine, minimize pressure losses, minimize inlet flow distortion and to match the inlet flow swirl to the compressor requirements. The detailed design of the inlet is a strong function of how the engine is integrated into the airframe. Raymer [Ref. 34] provides a good discussion on the types of buried and podded engines. It is the writer's opinion that a podded nacelle type would allow easy engine access for maintenance (lowers the MTTR). However a podded nacelle type engine would likely increase $C_{D,0}$ as compared with an buried fuselage engine. A pitot type inlet has the advantage of not being influenced by the flowfield of other aircraft components, but requires very long ducts and therefore increases weight and skin friction drag. The weight of a short duct length is given by Nicolai [Ref. 30] which suggests that the weight of a external turbofan cowl and duct is directly proportional to $L_d^{0.731}$, i.e. (subsonic duct length, per inlet, ft).

The Global Hawk podded engine is used as a reference in QFD Matrix 2. Therefore, a podded engine and inlet design is expected to result in lower weight, higher MTTR but higher $C_{D,0}$ and consequently lower $\left[\frac{L}{D}\right]_{\max}$.

10. Percentage of Composites

An aircraft designed using advanced composites may have the advantage of smaller overall design and less weight compared with metallic material. Composites also offer advantages of reduced number of fasteners, possible increased corrosion resistance and may have a better potential (than metal parts) for extended operational life. This increase in capability comes at an increase in cost [Ref. 33]. It is noted from Figure 12 that with greater than 50% composites utilization, the total cost airframe cost begins to increase. A few reasons for the potentially higher cost of composites are that the properties of these engineered materials frequently have to be verified. In addition,

because of the severe thermal cycling experienced in the autoclave, special tooling with good durability is required.

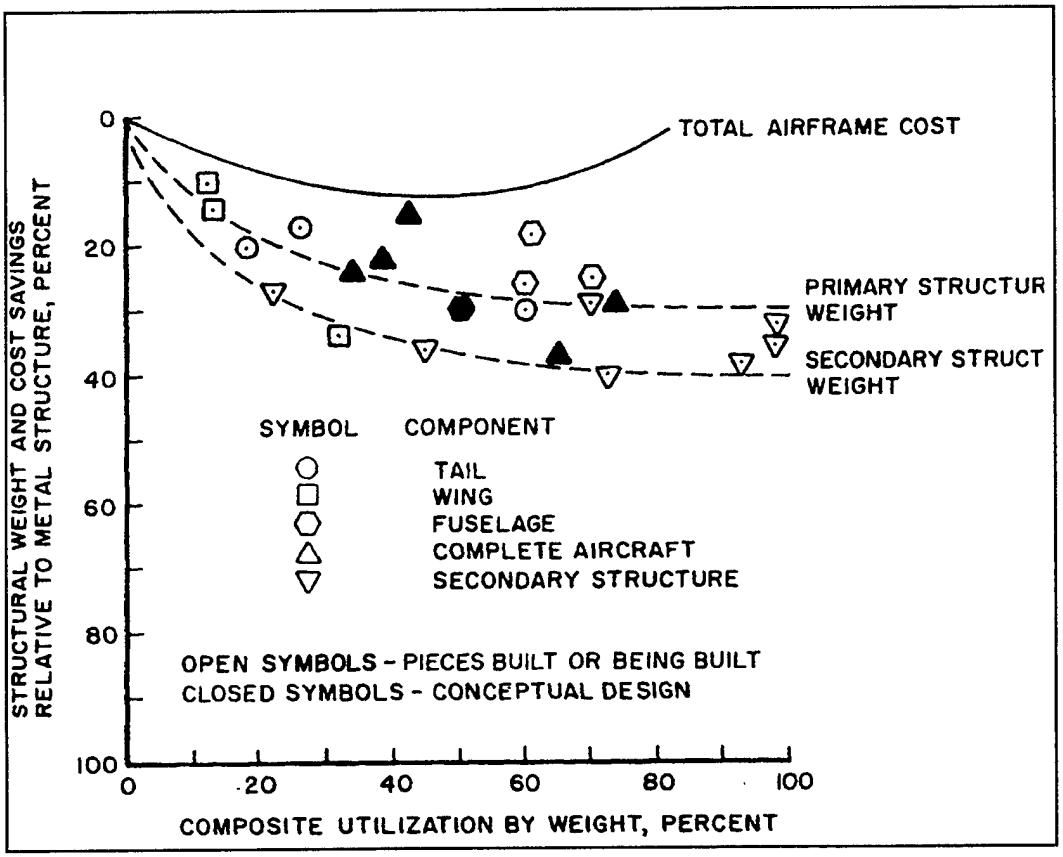

Figure 12. Weights and Cost Savings Using Composites. [From Ref. 30].

Due to better specific strength, a composite wing will also allow a higher AR with a lower t/c ratio. The flexural strength of a composite component is the resistance to breakage by bending stresses [Ref. 39]. A case in point is the Global Hawk UAV which has a graphite composite wing and empennage, but a conventional aluminum fuselage. In the writer's opinion, a lighter aircraft would also result in a lower T/W ratio and this could translate to needed a lower required design specific strength and stiffness. However, it is likely that the MTTR may be higher due to the complexities in repairing composites.

11. Fatigue

There are two distinct types of Stress Amplitude – Cycles behavior, or what is popularly termed the S-N curves, mentioned in Callister [Ref. 32]. Typical S-N curves are shown below in Figure 13. For some ferrous and titanium allows, a fatigue limit exists. This fatigue limit or endurance limit is the stress amplitude below which fatigue will not occur. This fatigue limit represents the largest value of fluctuating stress that will not cause failure for essentially an infinite number of cycles.

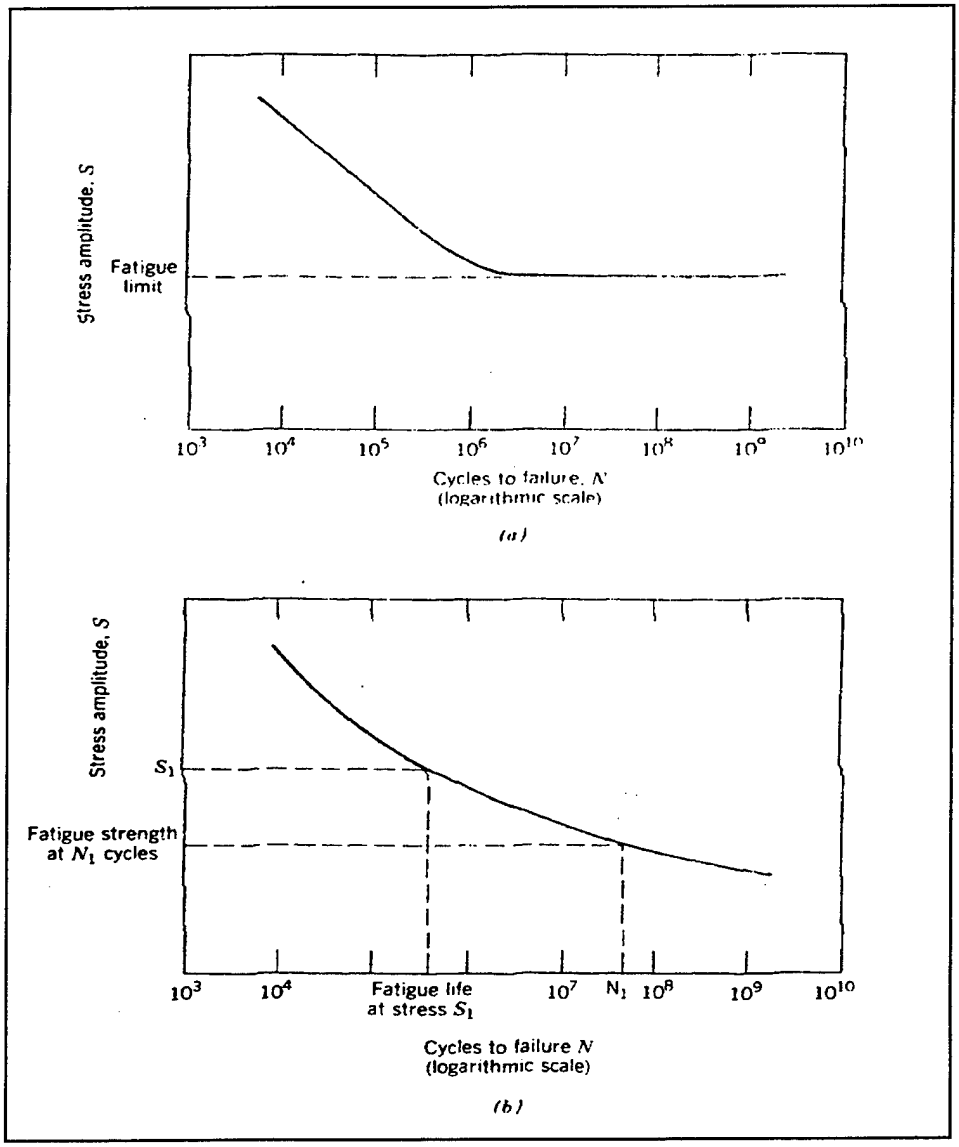

Figure 13. Typical S-N Curves. [From Ref. 32].

Most non-ferrous alloys, e.g., aluminum, do not have a fatigue limit, i.e., the S-N curve continues its downward trend to increasing N cycles. For these materials, the fatigue response is specified as fatigue strength. Fatigue strength is defined as the stress level at which failure will occur for some specified number of cycles. Another parameter, fatigue life is the number of cycles to failure at some specified stress level.

Figure 14 shows the comparison of fatigue strength of graphite, steel, fiber glass and aluminum. It illustrates the constant-amplitude fatigue for higher strength, lower-cost graphite-epoxy in tension-tension cycling. Figure 14 shows that graphite-epoxy composite material out-performs aluminum alloy in terms of fatigue strength (cycles to failure). The percentage of strength retention of graphite-epoxy exceeds that of the aluminum after 50,000 cycles. Figure 14 serves to reinforce the fact that composites are an attractive option for aircraft parts that are subject to fatigue stresses.

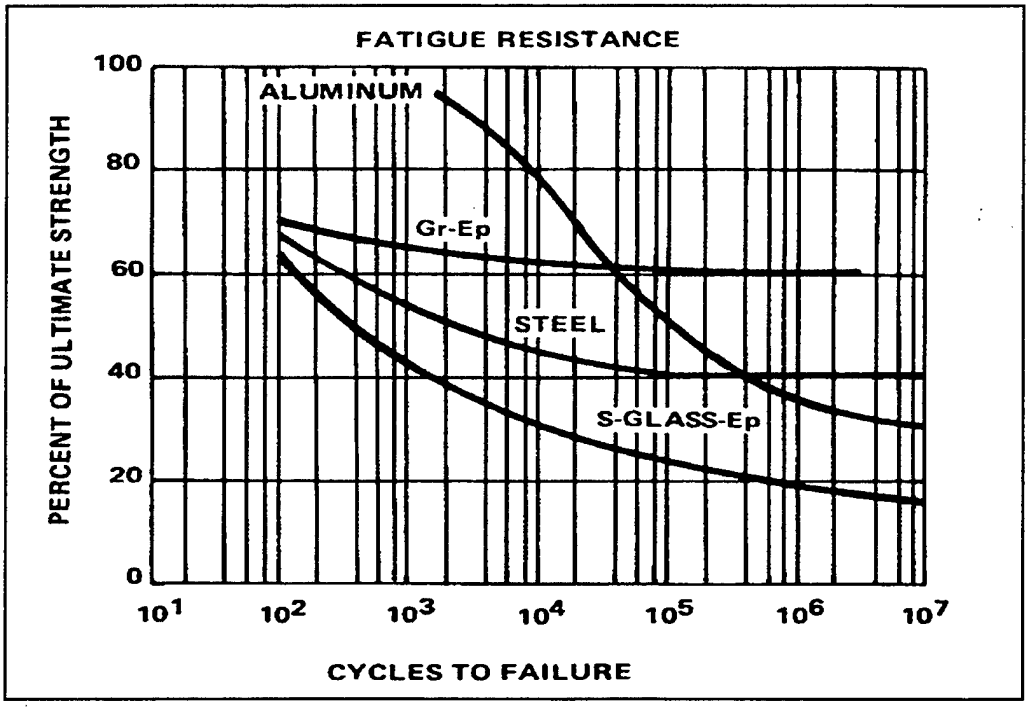

Figure 14. Fatigue Strength of Composites and Aluminum. [From Ref. 39].

12. Fuel Tank Volume

A long endurance UAV will require a large fuel volume capacity. This generally means a higher gross weight and a higher wing loading (for a constant wing area). It may be possible that the $C_{D,0}$ may increase if there are external tanks added to the HALE UAV design or if the fuselage volume is increased to attain sufficient fuel for range and endurance. Again, a higher $C_{D,0}$ would mean an eroded $\left[\frac{L}{D}\right]_{max}$. However, there is a positive relationship between a thicker airfoil and fuel tank volume since a thicker airfoil offers more fuel storage volume in the wing structures.

B. IMPACT OF QFD MATRIX 2

The relative importance of the performance parameters in QFD Matrix 2 are prioritized based on the weight importance computed from QFD Matrix 1. Then based on the literature survey and empirical relationships where available, the relationship matrix is scored. Trade studies suggested by the QFD Matrix 2 roof analysis is summarized in Table 8.

Parts Char.		Design Areas To Be Evaluated
Fineness Ratio ↑	Inlet Design Length ↓	A preferred longer fineness ratio needs to be evaluated against a shorter inlet design.
Fineness Ratio ↑	Fatigue ↑	A fatigue analysis is required as fineness ratio is increased, i.e. a longer fuselage may be more fatigue prone in terms of torsional and bending loads.

Table 8. QFD Matrix 2 Roof Analysis.

QFD Matrix 2 (see Figure 15) shows that the most important parts characteristics to be considered in meeting operational requirements are utilization of a high percentage of composites, a large airfoil thickness to chord ratio, a small wing sweep angle, a well-designed empennage and a wing with high fatigue strength. It is also suggested that

increasing the number of engines has an adverse effect on the aircraft design, and the design team would do well to design the aircraft with only one (highly reliable) engine.

It is noted that there are two design areas identified for trade studies as discussed in the QFD Matrix 2 roof analysis. This may be expected as the main aircraft design conflicts are upfront in QFD Matrix 1 where the key performance parameters affect one another more significantly then downstream deployments of QFD matrices. Thus, it may be concluded that cost savings appears to be most significant when the conceptual design is thoroughly deliberated and all trade-off studies are carefully weighed for the desired operational outcome.

QFD Parts Characteristics Matrix

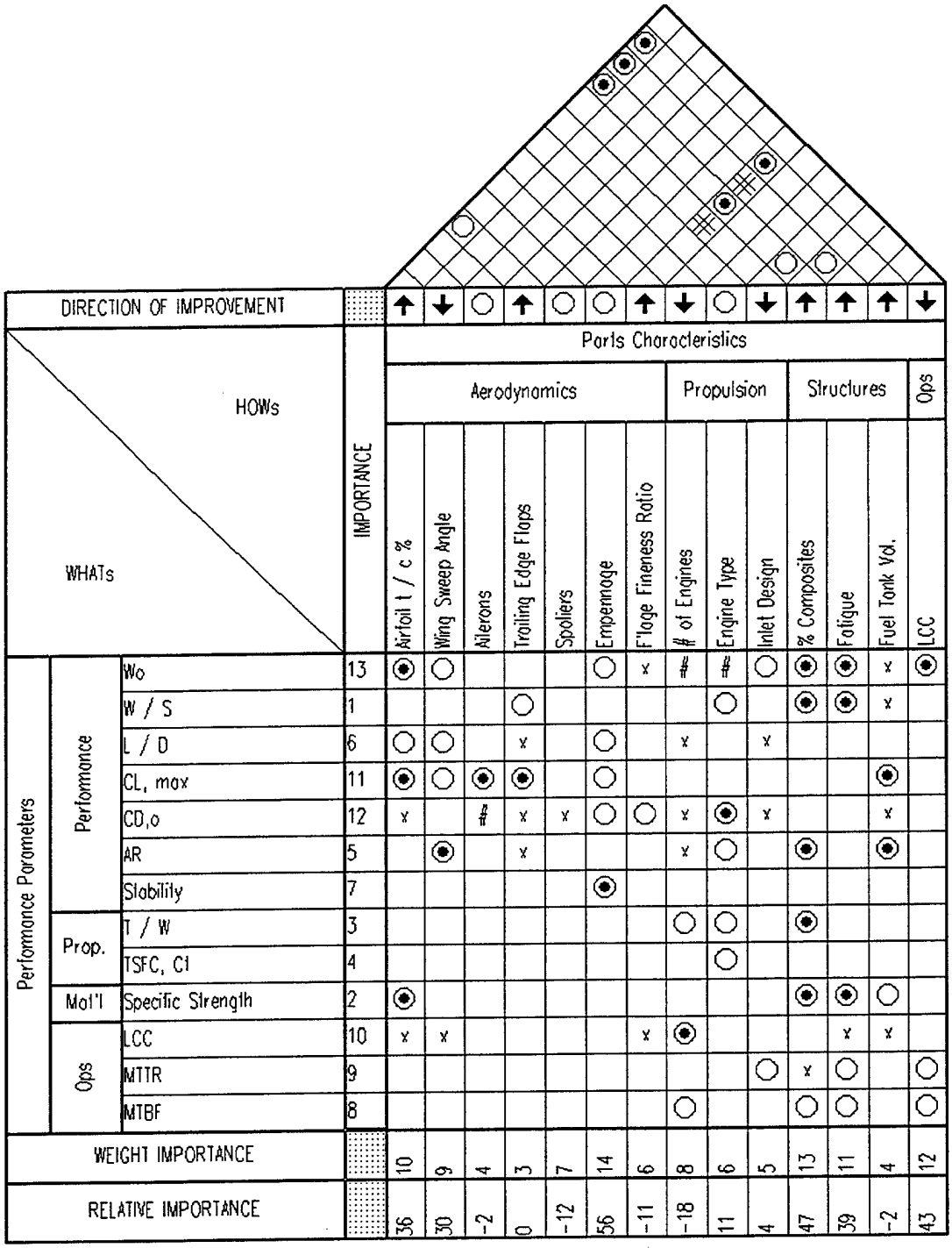

DIRECTION OF IMPROVEMENT				↑	↓	○	↑	○	○	↑	↓	○	↓	↑	↑	↑	↓
WHATs \ HOWs			IMPORTANCE	Parts Characteristics													
				Aerodynamics							Propulsion			Structures			Ops
				Airfoil t / c %	Wing Sweep Angle	Ailerons	Trailing Edge Flaps	Spoilers	Empennage	Flage Fineness Ratio	# of Engines	Engine Type	Inlet Design	% Composites	Fatigue	Fuel Tank Vol.	LCC
Performance Parameters	Performance	Wo	13	◉	○				○	×	#	#	○	◉	◉	×	◉
		W / S	1				○					○		◉	◉	×	
		L / D	6	○	○		×		○		×		×				
		CL, max	11	◉	○	◉	◉		○							◉	
		CD,o	12	×		#	×	×	○	○	×	◉	×			×	
		AR	5		◉		×				×	○		◉		◉	
		Stability	7						◉								
	Prop.	T / W	3								○	○		◉			
		TSFC, Ct	4									○					
	Mat'l	Specific Strength	2	◉										◉	◉	○	
	Ops	LCC	10	×	×					×	◉				×	×	
		MTTR	9										○	×	○		○
		MTBF	8								○			○	○		○
WEIGHT IMPORTANCE				10	9	4	3	7	14	6	8	6	5	13	11	4	12
RELATIVE IMPORTANCE				36	30	-2	0	-12	56	-11	-18	11	4	47	39	-2	43

Figure 15. HALE UAV QFD Matrix 2.

V. QFD MATRIX 3: DEPLOYING PART CHARACTERISTICS TO MANUFACTURING PROCESS CHARACTERISTICS

The third phase in the UAV conceptual QFD study is the deployment of part characteristics into possible or representative manufacturing processes. At this stage, one must be careful to constantly keep the customer attributes in mind as it is easy to lose the voice of the customer.

A. PROCESS PLANNING

The HALE UAV is a typically large and complex system, consisting of several major sub-systems, i.e. wings, fuselage, empennage, propulsion, etc. Having surveyed literature on design for manufacturing [Refs. 35 to 39], the writer is of the opinion that deploying the QFD matrices from parts to processes must be specific to the aircraft sub-system. For example, the wing as a sub-system, can be further broken down to longerons, ribs, stiffeners, integral wing tank, skin, ailerons, spoilers, flaps, etc. In QFD methodology, each of these wing parts can be deployed against manufacturing processes and subsequently deployed into production controls.

This specific-part to specific-process QFD Matrix is also adopted in the classic paper by Hauser and Clausing [Ref. 5]. This paper provides an excellent example in relating the importance of an extrusion speed of 100 rpm which helps gives a reproducible diameter for the weather-stripping bulb, resulting in good sealing without excessive door-closing force. This feature aims to satisfy the customer's desire for a "dry, quiet car with an easy-to-close door". The Hauser and Clausing paper [Ref. 5] showed how QFD can systematically translate a customer voice to a key manufacturing process and control. It is not the intention of this research effort to go into detailed manufacturing operations of each aircraft part at the conceptual stage. However, it is acknowledged that the detailed manufacturing process analysis is important and will impact the successful outcome of the customer attributes, and thus should be a design consideration.

Hence, the objective of QFD Matrix 3 process deployment will focus on deploying the key HALE UAV airframe parts, i.e., wing structure, airfoil t/c and contours, wing sweep, empennage design and general structural requirement. QFD Matrix 2 concluded that utilization of composites in the HALE UAV design significantly contribute to the customer requirements, QFD Matrix 3 will focus on the importance of composites fabrication techniques best suited for the key UAV parts. The QFD metal forming and machining matrices, also deemed important for any aircraft manufacturing, will also be considered in QFD Matrix 3. However, the discussion will be scoped for aluminum alloys as this material can be expected to dominate mostly any metal utilization in HALE UAV aircraft [Ref. 34].

It is interesting to note that conventional aluminum alloys (2000 and 7000 series: industry designation) are being replaced by aluminum-lithium alloys and titanium alloys, because of their higher strength-to-weight ratios. Forged parts are being replaced with powder metallurgy (P/M) parts that are manufactured with better control of impurities and microstructure. Also, advanced composite materials and honeycomb structures are replacing traditional aluminum airframe components. [Ref. 34].

The approach to developing QFD Matrix 3 is to deploy the key part characteristics against different composite manufacturing methods. The objective is to determine what is the most reasonable or probable manufacturing method for each part characteristic of the wing, fuselage and empennage system.

B. COMPOSITE DESIGN CONSIDERATIONS

Composite materials provide several advantages over metallic materials, e.g. tailoring the mechanical properties to meet specific design requirements, possible weight saving, corrosion resistance, etc. Raymer suggest that in a typical aircraft part, the direct substitution of graphite-epoxy composite for aluminum may yield a weight savings of 25 % [Ref. 34]. However, it is also noted that there are design concerns and inherent limitations of the two-phase, orthotropic material composition. For example, the fibers of

the composite are strong, stiff and thermally resistant while the composite matrix is generally weaker, less stiff and more susceptible to corrosion and solvents. The fiber-matrix inter-phase is also complex and can affect the toughness and damage tolerance of the composite. In essence, the structural designer must understand the properties of both fiber and matrix, make careful trade-offs to achieve the desired design outcome. For example, the designer has to evaluate and factor the higher stress concentrations at edges of drilled hole compared with metal aircraft parts. The inherent limitations of composites may also have negative impact on the design of structural attachments and joints. The fabrication of composites may result in delaminations which will have negative shear and compressive impacts on the structures. If a composite delamination of a critical length were to go undetected, the worst case scenario would be a crack propagation and an ultimate structural failure of the HALE UAV. [Ref. 33]. However, the design considerations of composite fiber and matrix are not covered in the scope of this thesis.

C. COMPOSITE FABRICATION PROCESS

To gain a better understanding of composite fabrication process, the writer carried out a literature survey which is summarized in Table 9 and 10. To better understand Tables 9 and 10, it is instructive to define some composite terminologies here. For example, Prepeg is ready-to-mold material in sheet form, which may be cloth, mat, or paper impregnated with resin and stored for use. The resin is partially cured and supplied to the fabricator, who lays up the finished shape and completes the cure with heat and pressure. Curing changes the properties of a resin by chemical reaction. Resin is a solid, semi-solid or pseudo-solid organic material which has an indefinite molecular weight, and exhibits a tendency to flow when subjected to stress. Resins are mostly polymers. Most current composite manufacturing methods can start by placing the uncured composite material into or onto a mold so that the material can be shaped into the final part. [Ref. 39].

Process	Description
Autoclave curing	The prepreg method generally uses both a vacuum and an autoclave to assist in consolidating and curing the part. Autoclaves allow the simultaneous imposition of heat, pressure and vacuum. Autoclaves can be as large as 25 ft. (8m) in diameter and 100 ft. (30m) in length. The major difficulty with autoclaves is the high capitalization cost because autoclaves are pressure vessels and are subjected to stringent pressure code regulations. However, because many parts can be cured simultaneously in an average autoclave, labor and cure costs on a per part basis need not be extremely high.
Elastic Reservoir Molding (ERM)	ERM produce sandwich components consisting of a rigid polyurethane, foam core with reinforcing face-sheets. This process can use existing hydraulic presses.
Thermoforming Thermoplastics	Thermoforming is a series of processes for forming thermoplastic sheet or film over a mold with the application of heat and pressure differentials. The process yields nearly finished parts. Typical parts may be complex but generally small, e.g. refrigerator liners, appliance housings and panels for shower stalls. Parts with opening or holes cannot be formed because the pressure differential cannot be maintained during forming.
Injection Molding	Injection molding produces parts by injecting a measured quantity of resin and chopped fiber into a molding die cavity that defines the shape of the part. Consolidation occurs under the application of heat and pressure. Injection molding is essentially a hot-chamber die casting. This process is also applicable to thermosets and thermoplastics. Molds are expensive. Typical parts are containers, electrical and communications components.
Hot Stamping	Hot stamping is akin to stamping of hot metal sheets. This process is suitable for chopped fiber reinforcements. Small to moderate size and complex shapes are possible.

Table 9. Summary of Composites Fabrication Processes - Part I.
[After Refs. 37, 38, 39].

Process	Description
Thermosets	Molding compounds with thermosets, when subjected to heat and pressure within the confines of a mold, cure or set into an infusible mass. An irreversible chemical change occurs. Part sizes of thermoset-molded parts vary from miniature insulators to large structural parts. Fiber-reinforced epoxies have excellent mechanical properties.
Pultrusions	This is a relatively low cost production method. Pultrusion employs continuous processing and uses prepegs or indirect impregnation. Continuous reinforcement fibers are impregnated with resin, shaped by drawing through a die and then cured. Its major limitation is that the cross-section normally must be constant. Long shapes with various constant profiles, e.g. rods or tubings may be made by pultrusion process. The product is cured during its travel through the die and cut into desired lengths. Pultruded parts are also used for pressure tanks, aircraft flooring, stringers and stiffeners in aircraft.
Filament Winding	Filament Winding can be wound as prepeg or run with direct impregnation. Axis-symmetric parts, e.g. pipes, as well as asymmetric parts are produced on a rotating mandrel. The reinforcing filament or tape is wrapped continuously around the form. The reinforcements are impregnated by passing them through a polymer bath. Part diameters ranging from 1 in. (23 mm) to 20 ft. (6 m) are common. The only limitations on size are those dictated by the geometries of the winding machine and the limitations in mandrel size and weight. Typical asymmetric parts are aircraft engine ducts, pressure vessels, fuselages, blades and struts.

Table 10. Summary of Composites Fabrication Processes – Part II.
[After Refs. 37, 38, 39].

The literature survey summarized in Tables 9 and 10 study provided input to QFD Matrix 3 regarding the selection of suitable composite manufacturing options for the key parts characteristics. Tables 9 and 10 suggest that autoclave curing and filament winding are probable choices for HALE UAV wing, fuselage and empennage parts as these composite manufacturing methods are able to accommodate large parts and are also established methods in current aircraft manufacturing industry [Refs. 36 and 39]. The RAND report [Ref. 33] on Advanced Airframe Structural Materials also has a good

discussion on composites manufacturing requirements, cost and suitability to varying design forms which are summarized in Tables 11 and 12.

Table 11 provides an overview of composite manufacturing process temperature and pressure control requirements. Also included are rough estimates of tooling, production and material costs. Each process is applicable to a limited number of materials, and the requirements of each material are in terms of temperatures and pressure controls. Table 11 provides input to QFD Matrix 3 on the tooling and production costs for all the composite manufacturing processes studied for the HALE UAV.

Process	Materials	Close Pressure Control	Close Temperature Control	Post Cure	Tooling Costs	Production Cost	Material Cost
Autoclave curing	Glass, Kevlar, graphite fabric; thermosets, thermoplastics	Yes	Yes	May be required with thermosets	High	High	Low to high; depends upon fiber/resin choices
Elastic reservoir molding (ERM)	Glass, Kevlar, graphite fabric; foams, epoxy resins	Yes	Yes	May be required	Low	Low	"
Thermoforming thermoplastics	Glass, Kevlar, graphite fabric; thermoplastics	Yes	Yes	No	Low	Low	"
Injection molding	Glass, graphite, chopped fibers; thermoplastics, thermosets	Yes	Yes	No	Depends upon part complexity	Low	"
Hot stamping	Glass, graphite, Kevlar fibers; thermoplastics, thermosets	Yes	Yes	No	Moderate	Low	"
Rapid cure thermosets	Glass, graphite, Kevlar fibers; thermosets	Yes	Yes	No			
Pultrusion	Glass, graphite, Kevlar fibers; thermoplastics	No	Yes	No	Low	Low	"
Filament winding	Glass, graphite, Kevlar fibers; historically with thermosets; thermoplastics developing	No	No	Some applications	Low	Low	"

Table 11. Process Manufacturing Requirements and Costs. [From Ref. 33].

The form and size of the part to be manufactured will put additional constraints on the applicable fabrication technique employed. Table 12 shows the suitability of certain manufacturing techniques to various typical aircraft parts forms. For example, medium to large parts such as wing and stabilizer skins, fuselage skins and doors can be fabricated using autoclave curing, elastic reservoir molding, thermoforming (thermoplastics), hot stamping or rapid cure (thermosets). Table 12 is a useful chart to suggest that autoclave curing and filament winding are good probable manufacturing choices for HALE UAV large integral structures, e.g., wing, fuselage and empennage.

	Form of Manufactured Component					
Process	Large Integral Structure[a]	Highly Contoured Parts[b]	Med/Large Plain Panels[c]	Closed Sections[d]	Open Sections[e]	Detailed Parts[f]
Autoclave curing	Yes	Yes	Yes	Yes	Yes	Yes
Elastic reservoir molding (ERM)	No	No	Yes	No	Yes	Possible
Thermo-forming thermo-plastics	No	No	Yes	No	Yes	No
Injection molding	No	No	No	Yes	Yes	Yes
Hot stamping	No	No	Yes	No	Yes	Simple Brackets
Rapid cure thermosets	No	No	Yes	Yes	Yes	Simple Brackets
Pultrusion	No	No	No	No	Yes	No
Filament winding	Yes	Yes	No	Yes	No	No

SOURCE: Mahon, personal communication, July 1989.

[a]Includes fuselage skins with stiffeners, wing skins with stiffeners, and bulkheads.

[b]Includes leading edges and fairings.

[c]Includes wing skins, stabilizer skins, fuselage skins, and doors.

[d]Includes closed hat section stiffeners, ducts, and piping.

[e]Includes stiffeners ("L" shaped and "Z" shaped), beams, ribs, and frames.

[f]Includes fittings and brackets.

Table 12. Suitability of Manufacturing Processes to Varying Forms. [From Ref. 33].

There was no information available on the Global Hawk on the specific areas of utilization of the graphite composites. However, Table 13 shows the graphite composition for a generic fighter and serves to suggest the trend of aircraft manufacturers to optimize the use of composites.

	Graphite Percent of Structure				
Component Type	10	25	35	45	55
Nonstructural access doors/panels	X	X	X	X	X
Structural access doors/panels	X	X	X	X	X
Vertical stabilizer skins	X	X	X	X	X
Horizontal stabilizer skins	X	X	X	X	X
Wing skins	X	X	X	X	X
Control surfaces	X	X	X	X	X
Speed brake	X	X	X	X	X
Landing gear doors	X	X	X	X	X
Additional doors/panels		X	X	X	X
Additional control surfaces		X	X	X	X
Spars, ribs		X	X	X	X
Shear webs, skin panels			X	X	X
Longerons				X	X
Frames, formers				X	X
Bulkheads					X

SOURCE: Aircraft contractor.

Table 13. Graphite Composition for a Generic Fighter. [From Ref. 33].

Figure 16 also shows an illustration of the usage of graphite composites on the F-16 is also found in Schwartz [Ref. 39]. It is anticipated that future designs of aircraft will inevitably include maximum use of composites.

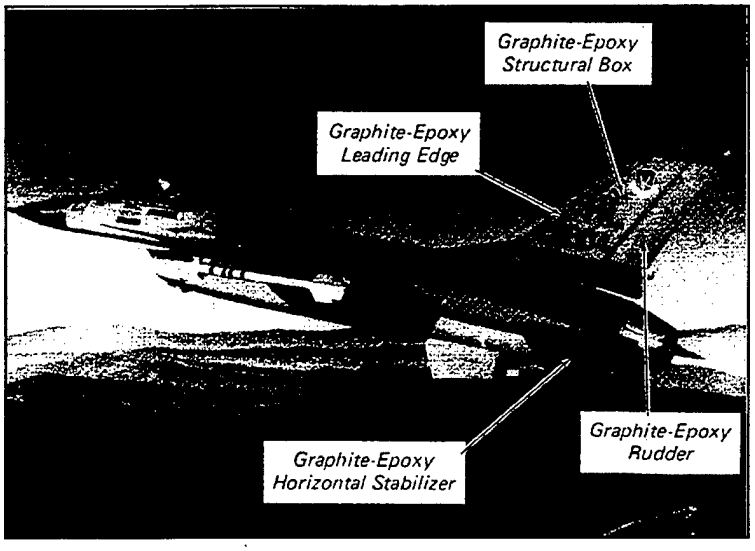

Figure 16. Utilization of Graphite-Epoxy in F-16. [From Ref. 39].

D. ALUMINIUM ALLOY FABRICATION

The most commonly used material in aircraft structures is aluminum alloys. Aluminum has an excellent strength-to-weight ratio, is easily formed, of moderate cost and resistant to chemical corrosion [Ref. 34]. For high-strength applications, the 7075 alloy is widely used. 7075 is alloyed with zinc, magnesium and copper. However it is interesting to note that 7075 is being replaced by the higher stress corrosion resistant 7049 and 7075 alloys in the Lockheed C-5A and C-5B. Since corrosion resistance is lessened by alloying, aluminum sheet is frequently clad with a thin layer of pure aluminum. [Ref. 34].

Bralla [Ref. 35] provides a good description of aluminum design methods for manufacturability. Structural shapes may be made by the extrusion process. Extrusion is a process whereby the material is forced through a die. Extruded parts may be round, rectangular or z-cross sections although other shapes can be drawn. Proper design and selection of die materials and lubricants are essential to obtaining a product with good quality and surface finish. Further finishing work will probably be required to achieve a good aircraft surface finish.

Forging is the process whereby the work-piece is shaped by compressive forces applied through various dies and tools. Forged parts have good strength and toughness, and are good for highly stressed and critical application, e.g., aircraft landing gear. The trend today is precision forging whereby the finished product is known as near net-shaped or net-shaped forging. Special dies allow greater accuracy in manufacturing and aluminum is a suitable material as it allows lower forging loads and lower temperature. [Ref. 35].

Milling is a process which a multi-tooth cutter rotates along various axes with respect to the surface of the work-piece. Milling machines in the aircraft manufacturing industry are usually computer numerical control (CNC) machines. These CNC machine tools have the ability to produce complex shapes with good dimensional accuracy, repeatability, reduced scrap cost, high production rates and product quality. Metal parts can also be made by compacting metal powders in suitable dies and sintering them (heating without melting). This process is called powder metallurgy (P/M). Powder metallurgy has become competitive with processes such as casting, forging and machining, particularly for relatively complex parts made of high strength and hard alloys. [Ref. 35].

The forming methods, discussed above, for aircraft structures in terms of process complexity, dimensional characteristics and tooling / production cost factors [Ref. 35] are summarized below in Table 14. In the writer's opinion, Table 14 suggests that forging and profile milling are probable methods for manufacturing large aircraft aluminum alloy parts employed in the wing, fuselage and empennage. Extrusions are limited to shapes (such as stringers) based on the die design, while powder metallurgy are limited to generally smaller parts (less than 75 mm).

Type of Part	Size and Complexity	Dimensional Characteristics	Cost Factors
Extrusions	Constant cross-sections of any length to about 7.5m are feasible. Cross section can be large enough to occupy a circle of 250 mm diameter in aluminum or 150 mm diameter in steel and can be very complex.	Tolerances for cross sectional dimensions range from $\pm$ 0.25 to 2.5 mm in aluminum, depending on the nominal dimensions.	Tooling is low in cost, making the process advantageous for moderately low quantities or more. Economies are gained when machining is avoided by the use of extended shapes.
Forgings	Closed-die forgings can be intricate, but secondary machining is normally required. The normal upper size limit is about 12 kg. Open-die forgings can produce much larger parts (up to 5 tons), but shapes are limited and secondary machining are required. Precision forging offers close tolerances. Machining are often not necessary and material utilization is very good.	Typical tolerances across the parting line run from 0.8 mm for small forgings of easily forged material like aluminum.	Tooling costs are moderate to high, depending on the complexity of the forging. Material loss is high because of flash and secondary machining. Labor costs are usually moderate. Forging is most economical for medium and high production levels. Precision forging requires high forces, intricate dies and tooling costs would be high.
Profile Milling	Milling is an effective means of removing large amounts of material and an efficient method of producing highly precise contours and shapes. It is a versatile process. Aircraft spars, ribs, fittings may be machine milled for precision [Ref. 36].	Surface finishes as low as 5μ m in have been obtained by milling. The number of parts to be produced before cutter or insert replacement is a major factor controlling the surface finish.	For numerically controlled mills, especially the bed types, offer increased rigidity and are capable of production accuracy on a continuing-production basis without frequent adjustment. Tooling costing in such instances can range from modest to quite high levels.
Powder Metallurgy (P/M)	Although size and weight are limited, the process is capable of producing relatively complex parts economically, in net shape form to close tolerances. P/M parts are normally small (less than 75 mm).	High dimensional control. Tolerances range from $\pm$ 0.006 mm in small bores to $\pm$ 0.13 mm in larger dimensions.	The P/M process is suitable for medium to high volume production and has competitive advantages over casting, forging and machining. High production rate on relatively complex parts. Tooling costs are high and labor costs are low.

Table 14. Summary for Forming Methods for Aircraft Structures. [After Ref. 35].

E. TITANIUM AND ITS ALLOYS

For QFD Matrix 3, only composites and aluminum are considered. However, as titanium is considered an important metal in the aerospace industry, it shall be briefly covered here. Bralla [Ref. 35] provides a good discussion of titanium and its alloys. Titanium is considered a light metal relative to steel. It possesses excellent corrosion resistance property and a low thermal coefficient of expansion. Titanium is widely used in the aerospace industry in propulsion components such as compressors and turbines.

F. IMPACT OF QFD MATRIX 3

The manufacturing literature survey by the writer provides data to complete QFD Matrix 3. If the intended material utilization for the HALE UAV parts is largely composite, it is critical to ensure that the designed mechanical properties of the composite parts are achieved by ensuring a suitable and correctly placed fiber as well as matrix selection considerations. The QFD deployment suggests that autoclave and filament winding are the most probable composite manufacturing methods for HALE UAV large integral and highly contoured parts. A detailed and separate study outside the scope of this thesis, is recommended to decide whether or not, if over the production run, filament winding is more cost-effective than autoclaving. As for the aluminum alloy components, QFD Matrix 3 shows that milling and precision forging are possible manufacturing methods that the design team should consider as good manufacturing options.

QFD Matrix 3 (see Figure 17) also suggests that manufacturing processes like Elastic Reservoir Molding, thermo-molding, injection molding, hot stamping, rapid cure thermosets and pultrusion have no relationships with the HALE UAV parts characteristics. The reason is that these manufacturing methods are more suitable for smaller parts (as discussed in Tables 9 through 12). It is also noted that there is no relationship in the QFD Matrix 3 roof as each manufacturing process was considered to be independent of other processes.

QFD Manufacturing Processes Matrix

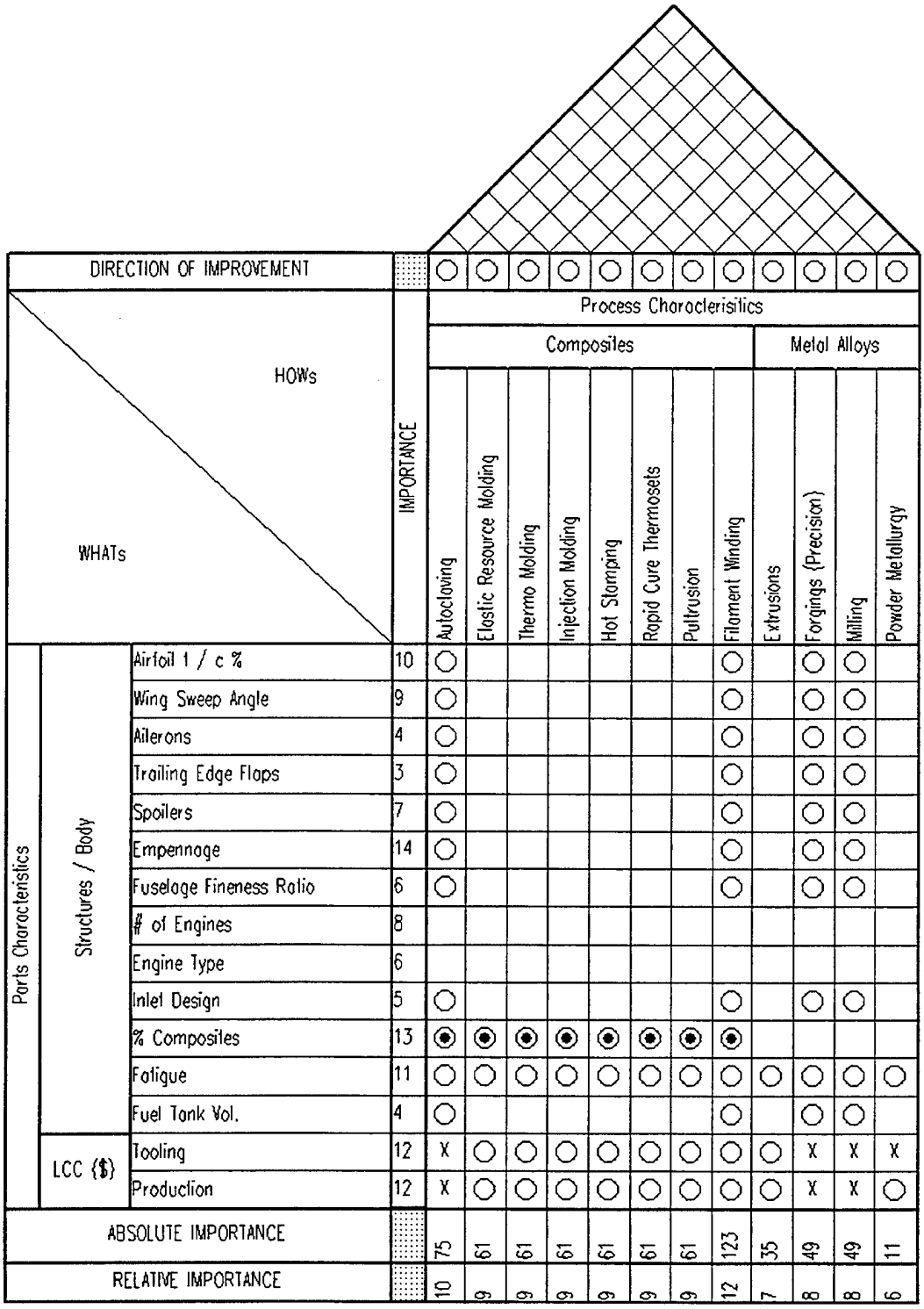

Figure 17. HALE UAV QFD Matrix 3.

This page is intentionally left blank.

VI. QFD MATRIX 4: DEPLOYING PROCESS CHARACTERISTICS TO MANUFACTURING OPERATIONS CONTROLS

QFD Matrix 3 suggested that the probable manufacturing processes to meeting the HALE UAV parts characteristics were autoclave molding and filament winding for composite parts, while milling or precision forging are potential methods for aluminum parts. The objective of this QFD phase, i.e. QFD Matrix 4, is to deploy the manufacturing methods for composites and aluminum to determine the manufacturing operations controls for the HALE UAV production.

A. CONTROLS IN COMPOSITE FABRICATION

The mechanical properties of composite materials are dominated by the fibers. Fibers are able to withstand greater stresses than metals because of the fiber and matrix interaction thus resulting in the redistribution of stresses. This higher strength in turn depends on the effectiveness of the bonding between the fibers and the matrix. Thus, it is important to place great emphasis on the manufacturing controls to ensure the desired bonding is achieved. To this end, two key composite processes will be discussed.

Autoclave molding is a combination of a vacuum-bag and pressure-bag molding. The lay-up (component materials of a laminate) is bagged and evacuated in the vacuum-bag process to remove trapped air or other volatiles. While under vacuum, it is exposed to heat and high pressure in an autoclave to produce the most dense parts. The vacuum and autoclave pressure cycles are adjusted to permit maximum removal of air without incurring excessive resin material flow. Curing pressures are normally in a range of 50 to 100 psi. [Ref. 39].

A typical autoclave consists of a large cylindrical metal pressure vessel pressurized with air and/or carbon dioxide, thermally insulated, steam-heated with forced circulating hot air, and a large circular door at the end of the autoclave vessel [Ref. 39]. A typical autoclave system is shown in Figure 18. Schwartz [Ref. 39] discusses the

minimum requirements for a typical autoclave system. The curing controls critical to the quality of the part are temperature control, air circulation to maintain specific curing temperature of $\pm 15\ ^0F$ ($8.3\ ^0C$), high capacity pressurization (usually does not exceed 100 psi) and a vacuum control. The literature survey [Refs. 37, 38 and 39] by the writer on composites manufacturing did not indicate which of the controls are more important.

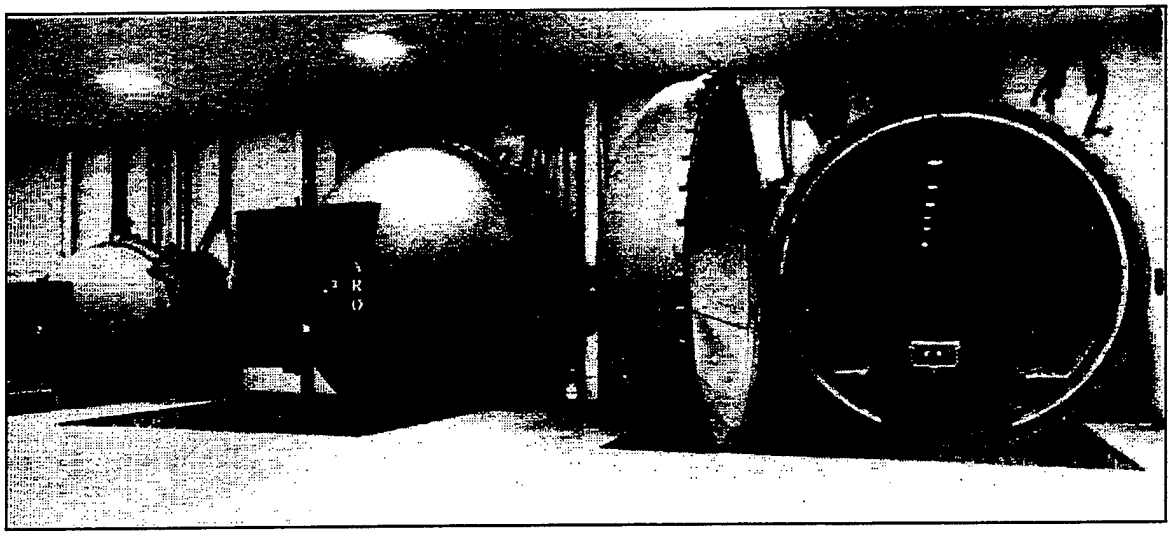

Figure 18. A Typical Autoclave System. [From Ref. 39].

Filament winding is a simple and effective method for producing bodies of revolution in a wide range of sizes. Part diameters ranging from 1 in. (23 mm) to 20 ft. (6 m) are common. The process consists of wrapping bands of continuous fiber or roving over a mandrel in a single machined-controlled operation. At present, wet winding is the most common method for reasons of low cost. Producers equipped with resin formulating facilities have the flexibility of resin formulation to meet specific requirements for different parts [Ref. 39]. In wet winding, the tension of the roving must be adjusted as the diameter of the part increases for accurate control of the resin/reinforcement ratio. Viscosity and pot life of the catalyzed system are also important processing considerations. The pot life is the length of time a catalyzed resin system retains a viscosity low enough to be used in processing. A catalyst is a substance which changes the rate of a chemical reaction without itself undergoing permanent

change in its composition. A low viscosity of the resin is required for complete wet-out of the strands and for removal of trapped air. A pot life of at least several hours is required, since it is not generally advisable to wind over-gelled or partially gelled resin. Gel time and flow behavior are also important factors. In some cases, there is also a limit on temperatures, as lining materials deteriorate above this particular temperature. A typical filament winding process is shown in Figure 19.

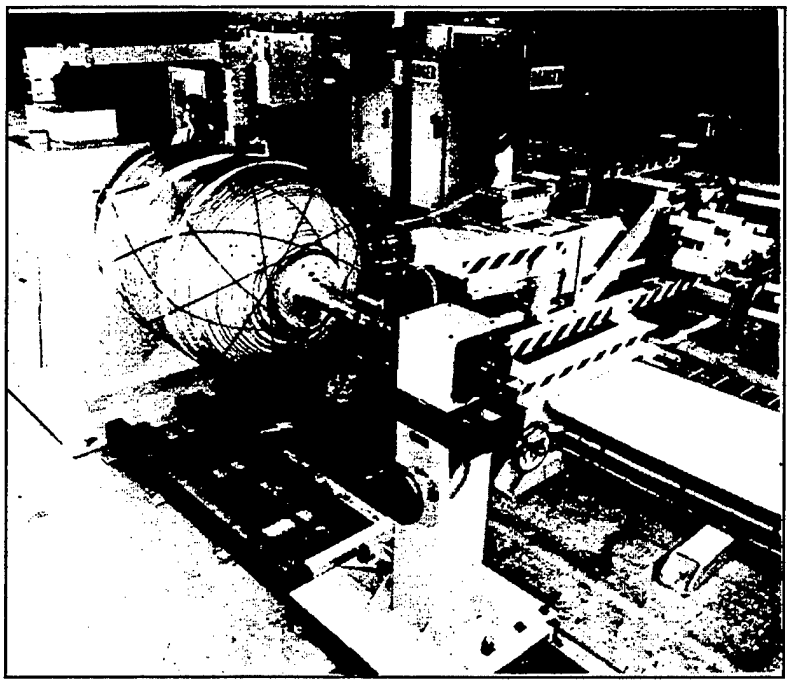

Figure 19. A Typical Filament Winding Process. [From Ref. 39].

B. INSPECTION OF COMPOSITE DEFECTS

Many defect types can affect the quality of a composite structure and no single nondestructive test can find and isolate all of them [Ref. 33]. Common defects include delaminations, foreign matter (inclusions), high porosity, honeycomb core damage, moisture, fiber breaks and matrix cracks. These defects may be the result of inadequate manufacturing controls or poor workmanship. The RAND report [Ref. 33] summarized the sensitivity of Non-Destructive Inspection (NDI) methods to different flaw types.

Each NDI method has its limitations. Table 15 describes the sensitivity of some NDI methods to different flaw types. There are three levels of categorization of sensitivity, i.e. VG, G and L as explained in the legend of Table 15.

	NDI Method								
Flaw Type	Ultrasonic Transmission[a]	X-ray Radiography	Neutron Radiography	Laser	Thermal Infrared	Tap Test	Acoustic[b]	Eddy Current	Visual
Porosity	VG/G	VG	L	—	—	—	G	—	—
Foreign material	VG/G	G	L	—	L	—	—	—	—
Delamination	VG	—	—	—	G	—	L	—	—
Matrix cracks	L	G	—	—	—	—	G/L	—	—
Fiber breaks	—	VG	—	—	—	—	G	G	—
Impact damage	G/L	—	—	G	G	G	L	—	L
Skin/skin disbond	VG/G	G	G	VG	VG	VG	—	—	—
Skin/core disbond	VG/G	L	L	VG	VG	G	G	—	—
Core damage	VG	VG	—	G	G	—	—	—	—
Water intrusion	L	G	VG	L	L	—	G	—	—

SOURCE: Meade, 1988.

[a]Ultrasonic transmission includes four types of tests: through transmission, pulse echo, angle, and resonance.

[b]Acoustic includes two types of tests: emission and ultrasonic.

— not applicable.

VG: Good sensitivity and reliability; good candidate for primary method.

G: Less reliability or limited applicability; may be good backup method.

L: Limited applicability; may provide some useful information.

Table 15. Sensitivity of NDI Methods to Different Flaw Types. [From Ref. 33].

The inspection of composite defects can be complicated as there may be several types of defects present in the manufactured part. To add to the complication, each NDI technique is not sensitive, or has limited sensitivity to each type of flaw. Thus, depending on the criticality of the aircraft part, more than one NDI technique is needed. Table 15 shows that Ultrasonic NDI is sensitive to nine out of ten flaws listed.

C. MANUFACTURING CONTROLS IN ALUMINIUM PART FABRICATION

Positioning accuracy in NC machines is defined with respect to how close the machine can be positioned to a certain coordinate system. An NC machine usually has a positioning accuracy of at least ± 3 μm (0.0001 in.) [Ref. 35]. Hence, the importance of repeatability, which is defined as the closeness of agreement of repeated position

movements under the same operating conditions of the machine. Repeatability is about ± 8 μm (0.0003 in.). Another control factor is resolution, defined as the smallest increment of motion of the machine components. This is about 2.5 μm. The factors for maintaining these accuracies are ensuring that a sufficiently high stiffness of the milling machine tool and that the backlash of the gear drives are eliminated. Also, rapid response to command signals that incur friction and inertia must be minimized.

In precision forging, special dies allow parts to be machined to greater accuracies. The process requires higher capacity equipment because of the greater compressive forces required to achieve the accuracies and details of the design. Aluminum, in particular, is suitable for precision forging employment due to lower compressive forces and temperature requirements to forge the material. Consequently, the wear on the forging die is minimal and product surface finish is good. Precision forging requires special dies, precise control of material volume and shape, and proper positioning of the part in the die cavity [Ref. 37].

D. SUMMARY OF PROCESSES CONTROLS

The process controls leading to the desired manufacturing outcomes are shown in Table 16.

Process	Manufacturing Controls	Desired Results
Composites		
Autoclave	1. Temperature control 2. Air circulation 3. Pressurization 4. Vacuum control	Designed Bonding Strength and consequent mechanical properties.
Filament Winding	1. Tension of roving 2. System Viscosity 3. System Pot life	Designed Bonding Strength and consequent mechanical properties.
Aluminum		
Milling	1. Machine tool stiffness 2. No backlash of gear drives 3. Minimized friction and inertia in tool response	Repeatability in tool movements and high resolution in tool incremental movement.
Precision Forging	1. Design of special dies 2. Control of material volume and shape 3. Positioning of part in the die cavity	Near-net shape product

Table 16. Summary of Key Manufacturing Controls. [After Refs. 37, 38, 39].

E. IMPACT OF QFD MATRIX 4

QFD Matrix 4 (see Figure 20) suggests the critical manufacturing operation control parameters that are important in order to achieve the desired quality of the aircraft parts. The manufacturing QFD phase forces the design team to ensure that the design considerations towards meeting the customer requirements are achievable and practical in the manufacturing environment.

Based on the writer's literature survey, it appears that the filament winding method may be more cost effective compared with the autoclave method for the manufacturing of the HALE UAV wing, fuselage and empennage. Of course, the cost comparison has to be validated in actual trade studies. Thus, in the QFD Matrix 4 "Importance" column, the filament winding is prioritized higher than the autoclave. As for aluminum alloy fabrication, based on the writer's observation on an Naval Postgraduate School field trip [Ref. 36], it appears that milling is preferred in the industry and therefore prioritized higher than forging in the QFD Matrix 4. Also, in the writer's opinion, NDI is absolutely critical as a quality assurance check and especially so for the composites parts. Further study is needed to determine if ultrasonic NDI methods are sufficient or is there a need to further complement with other NDI methods.

The outcome of QFD Matrix 4 is the recognition that the important manufacturing parameters, e.g. temperature and vacuum control in the autoclave method are carefully planned for, controlled and achieved in order to ultimately achieve the requirements of the customer attributes. The roof analysis also suggests a potential trade study area for critical control in the autoclave method. The pressurization and the vacuum control aspects of autoclaving require conflicting controls. These parameters should be evaluated and controlled critically during the curing process. The "Absolute Importance" row of QFD Matrix 4 suggests that process control parameters such as NDI, roving tension and viscosity be accorded higher priorities that other parameters.

QFD Process Controls Matrix

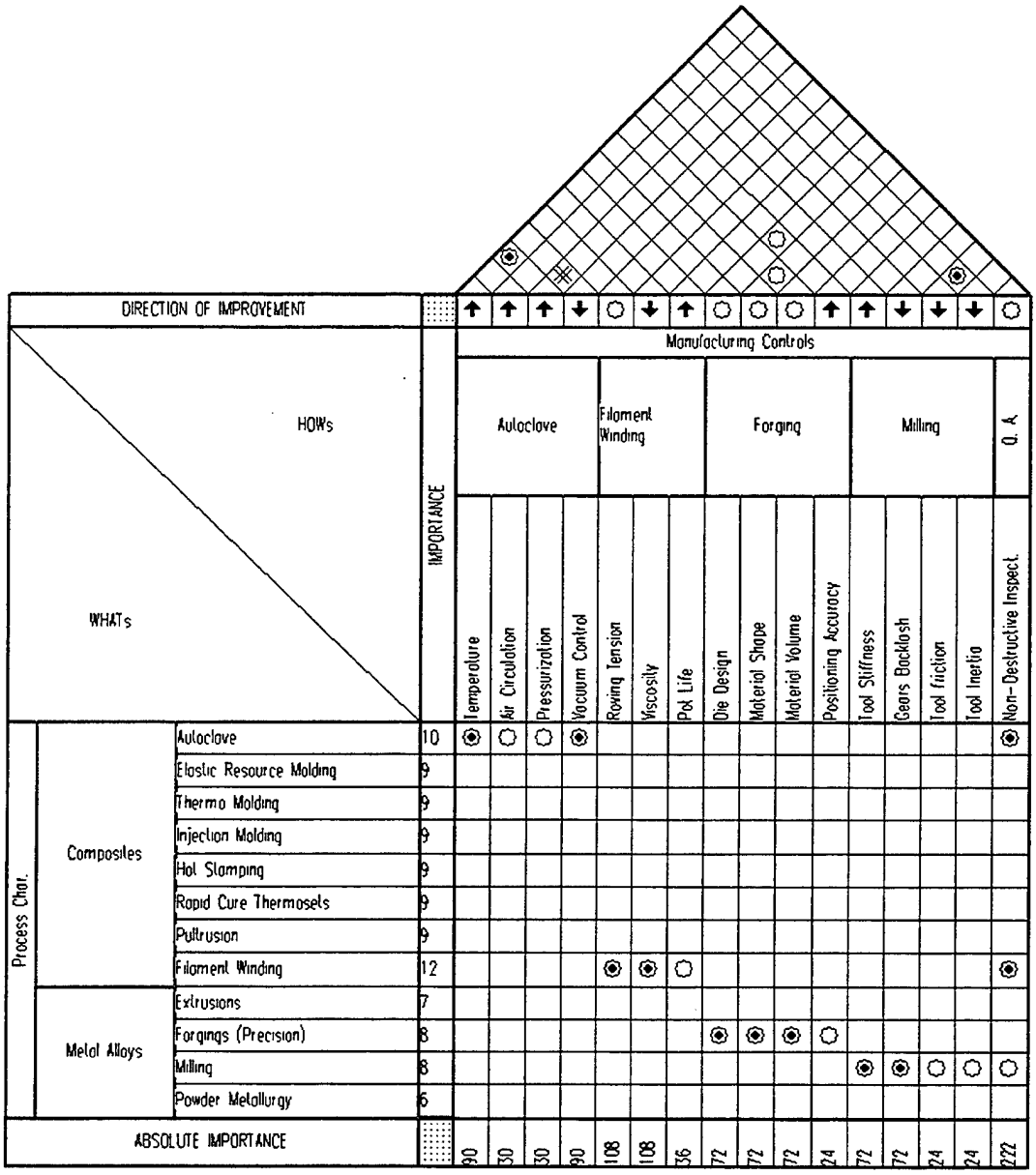

Figure 20. HALE UAV QFD Matrix 4.

This page is intentionally left blank.

VII. CONCLUSIONS

The Four-Level QFD model discussed herein, i.e., performance parameters, part characteristics, manufacturing processes and process controls have been applied to the conceptual configuration development of a HALE UAV. The customer attributes are typically drawn from a Request-for-Proposal and translated into UAV performance parameters. The performance parameters are prioritized and design areas for trade studies are identified. The UAV part deployment phase identified the important part characteristics which were evaluated to best meet the performance parameters. Then probable manufacturing processes are selected for the fabrication of composite and aluminum UAV parts. Finally, the probable manufacturing processes are analyzed to identify process controls to ensure a quality product.

The strength of the four-level QFD analysis is that it requires the design team adopt a system integration approach at the earliest stage in conceptualizing the aircraft design configuration to determine which design criteria are important in meeting the customer voice or attributes. The customer voice has to be clearly understood and translated to measurable UAV system performance parameters. Design conflicts are identified early for in-depth trade-off studies. Negative values in the QFD matrices highlight the opportunities for break-through design approaches. For example, the weight of the UAV has a high negative value as it has an adverse impact on the many customer attributes, e.g., endurance and range. QFD Matrix 1 shows that to reduce the overall UAV weight, the design team has to look at the wing, fuselage and empennage design parameters in terms of increasing airfoil thickness, maximum utilization of composites, fuel tank capacity, minimal wing sweep, etc. In addition, the design team has to also consider the feasibility of their design in terms of cost, manufacturability and process controls in ensuring that the HALE UAV performance parameters are achieved. In essence, applying the four-level QFD model permits a total and integrated approach to product, process and quality assurance design.

In essence, the four-level QFD model presented herein shows that to achieve the customer attributes of maximum endurance, range, cruise altitude and payload, the important performance parameters are low gross weight, low $C_{D,0}$, high $C_{L,\max}$ and a low life cycle cost. The part characteristics QFD matrix suggest a need to maximize utilization of composites, thick airfoil, high wing fatigue strength and low wing sweep. To achieve the part characteristics, the manufacturing methods considered were autoclave curing, filament winding, milling and precision forging. Figure 21 is an attempt to summarize the 'big picture", utilizing QFD methodology to provide a means to a powerful, systematic and structured approach to the design and development of a HALE UAV.

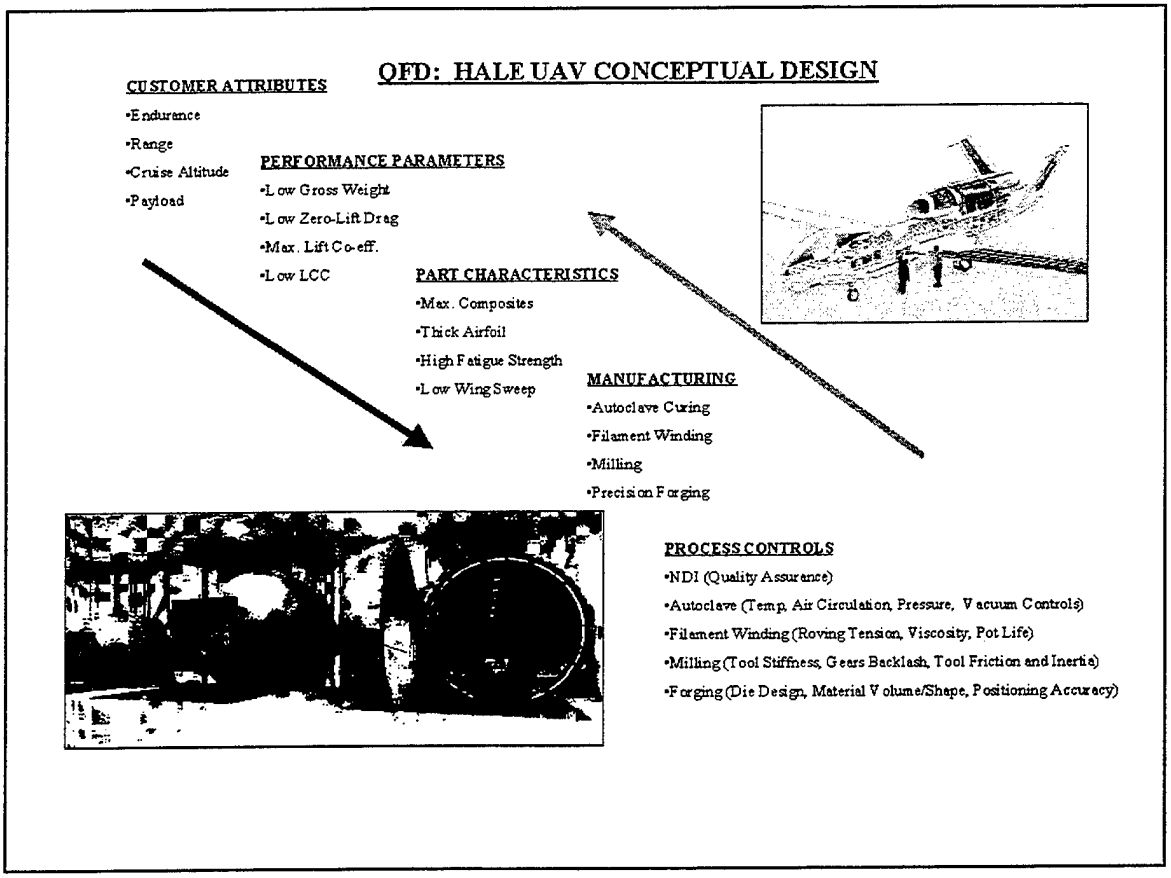

Figure 21. Areas of Emphasis in HALE UAV Design.

VIII. RECOMMENDATIONS

A. INTEGRATED TEAM APPROACH

This thesis effort is based on the writer's research and guidance from faculty members. It is believed that an integrated team approach will certainly allow a thorough coverage of every UAV design aspect, i.e., avionics, weights, structures, stability and controls, propulsion and intake design, life cycle costing, maintainability and so on. It is recommended that this research effort be used as an introduction to QFD in the Systems Engineering course in Aeronautical Engineering Department, and be used as a powerful and integrative approach in the capstone aircraft design class.

B. VALIDATE MANUFACTURING AND PROCESS CONTROLS QFD MATRIX

The QFD Matrix 3 and 4 are largely based on existing text book literature, discussions with thesis advisors and observations on a field trip [Ref. 36]. As a result, the writer also faced difficulties when attempting to validate the QFD design guide template in the areas of manufacturing with the industry. Future research effort may be to work with aviation manufacturing industries to validate and improve Matrices 3 and 4.

This page is left intentionally left blank.

APPENDIX A: MATLAB PROGRAM FOR CD0 ESTIMATION

The MATLAB code in Appendix A is to estimate the $C_{D,0}$ of the HALE UAV. The equations are drawn from the USAF DATCOM shown in the AA 2036 course notes, Aeronautical Curriculum 610.

```
% CD0 UAV Configuration Analysis
% Saved as Thesis/CD0_uav.m
% Major Rendell Tan - Thesis
clc
clear

% Parameters

% CDO of Main Wing
tc = .16; % thickness ratio of wing
V = 683.5; % freestream velocity (ft/s)
nu = 5.056e-4; % viscosity (ft^2/s)
ct = 2.25; % tip chord (ft)
cr = 8.4; % root chord (ft)
lambda = ct/cr; % taper ratio
c = 2/3*cr*(1+lambda+lambda^2)/(1+lambda); % mean aerodyn chord
Re = V*c/nu; % Reynolds Number
Cf = .455*(log10(Re))^-2.58; % Ave. Turbulent Skin Friction Coeff
CD0mainwing = 2*Cf*(1+2*tc+100*tc^4), % CD0 of Wing. Eqn 4.1.5.1a


% Wing Planform Area (given from Teledyne Ryan)
Sfpw = 540; % wing area (ft^2)


% CD0 of Fuselage
Lb = 44.4; % length of fuselage (ft)
dmax = 9.12; % max diameter of fuselage (ft)
dbase = 2;% base diameter (ft)
Re = V*Lb/nu; % Reynolds Number
Cf = .455*(log10(Re))^-2.58;% Ave. Turbulent Skin Friction Coeff
FR = Lb/dmax; % fineness ratio
disp('fineness ratio: '); % display fineness ratio
disp (FR);
SwSb = input('Sw/Sb: '); % Look up chart Fig. 2.3.3 USAF S&C DatCom
Sb = pi*(dmax/2)^2; % frontal area of fuselage (ft^2)
CD0skinf = 1.02*Cf*(1+(1.5/(Lb/dmax)^1.5)+(7/(Lb/dmax)^3))*SwSb; % CDO
Skin Friction eqn 4.2.3.1b
CD0base = 0.029*(dbase/dmax)^3/sqrt(CD0skinf);% base pressure CD0 eqn
4.2.3.1b
CD0fuselage = (CD0skinf+CD0base)*(Sb/Sfpw), % CD0 of Fuselage

% CD0 of Isolated Horizontal Tail
```

```
Crh = 4.8; % hor. tail root chord (ft)
Cth = 2.4; % hor. tail tip chord (ft)
toch = 0.16; % hor. tail thickness ratio
Bh2 = 7.2; % hor. tail half span
lambdah = Cth/Crh; % hor. tail taper ratio
cbh = (2/3)*Crh*((1+lambdah+lambdah^2)/(1+lambdah)); % c bar - hor.
tail mean aerodyn chord (ft)
Re = V*cbh/nu; % Reynolds Number
Cbfh = 0.455*(log10(Re))^(-2.58); % hor. tail ave. turbulent skin
friction coeff.
CD0h = 2*Cbfh*(1+(2*toch)+(100*toch^4)); % CD0 of hor. tail area prior
to
% Multiplication of Hor. Tail Wing Area Ratio eqn. 4.3.3.1a


% Horizontal Tail Planform Area (given)
Sfpht = 42.8; % hor. tail area (ft^2)
% Therefore;
CD0hortail = CD0h*Sfpht/Sfpw, % CD0 of Horizontal Tail


%-------------------------------------------------------------------------
% Summing Up the Total Aircraft Configuration CD0
Total_Config_CD0 = CD0mainwing + CD0fuselage + CD0hortail, % Total CD0

% Results Printed Below:
CD0mainwing =      0.0086

fineness ratio:    4.8684

Sw/Sb: 19.5

CD0fuselage =      0.0068

CD0hortail =       7.3779e-004

Total_Config_CD0 = 0.0161
```

APPENDIX B: MATLAB PROGRAM FOR CONSTRAINT DIAGRAM.

```
% High Altitude Long Endurance UAV Constraint Analysis
% MAJ Rendell Tan - Thesis
% Saved as qfd_constraint_2.m
clear all
%************************************
% Constants
% Maximum Thrust to Weight for Charts
TtoWMax = 0.6;

% Initial Estimates
CD01 = 0.0161; % Coeff of Drag at Zero Lift
AR1 = 25;    % Aspect Ratio
CL1 = 1.60; % Max Coeff. of Lift
e = 0.9; % Oswald Eff. Factor
K1 = 1/(pi*e*AR1); % K ratio


% Wing Loading Range from 0 to 100
nPts = 150;
WtoS = [0:1:nPts];
%************************************
% Mission #1 Take Off Ground Roll

TakeOff1 = zeros(nPts);
for WtS = 1:nPts
   TakeOff1(WtS) = (0.00424*WtS)/CL1;
end

figure
hold
plot(TakeOff1)
hold
axis([0,nPts,0,TtoWMax])
title('Take Off Ground Roll')
xlabel('Wto/S ~ Wing Loading (takeoff) ~ lbf/ft^2')
ylabel('Tsl/Wto ~ Thrust (sea level) to Weight (takeoff) Ratio')
%************************************

%************************************
% Mission #2 Constant Altitude / Speed Cruise
% Mission #3 Constant Speed Climb (same equation)

Casc1 = zeros(nPts);
for WtS = 1:nPts
   Casc1(WtS) = (0.283*K1*WtS)/AR1 + (354.94*CD01)/WtS;
end

figure
hold
plot(Casc1)
hold
```

```
axis([0,nPts,0,TtoWMax])
title('Const Altitide Speed Cruise')
xlabel('Wto/S ~ Wing Loading (takeoff) ~ lbf/ft^2')
ylabel('Tsl/Wto ~ Thrust (sea level) to Weight (takeoff) Ratio')
%************************************
% Mission #4 Sustained Turn, n = 3 g's

figure
WtoS = [0:1:nPts];

SusTurn1 = zeros(nPts);
for WtS = 1:nPts
   SusTurn1(WtS) = (0.543*K1*WtS)/AR1 + (554.72*CDO1)/WtS;
end


hold
plot(SusTurn1)
hold
axis([0,nPts,0,TtoWMax])
title('Sustained Turn')
xlabel('Wto/S ~ Wing Loading (takeoff) ~ lbf/ft^2')
ylabel('Tsl/Wto ~ Thrust (sea level) to Weight (takeoff) Ratio')
%************************************
%************************************
% Mission #5 Maximum Speed

figure
WtoS = [0:1:nPts];

MaxV1 = zeros(nPts);
for WtS = 1:nPts
   MaxV1(WtS) = (18491*K1*CDO1)/WtS;
end

hold
plot(MaxV1)
hold
axis([0,nPts,0,TtoWMax])
title('Maximum Speed')
xlabel('Wto/S ~ Wing Loading (takeoff) ~ lbf/ft^2')
ylabel('Tsl/Wto ~ Thrust (sea level) to Weight (takeoff) Ratio')
%************************************
%************************************
% Mission #6 Acceleration

figure
WtoS = [0:1:nPts];

Accel1 = zeros(nPts);
for WtS = 1:nPts
   Accel1(WtS) = (0.27*K1*WtS) + (355*CDO1)/WtS + .035;
end
```

```
hold
plot(Accel1)
hold
axis([0,nPts,0,TtoWMax])
title('Acceleration')
xlabel('Wto/S ~ Wing Loading (takeoff) ~ lbf/ft^2')
ylabel('Tsl/Wto ~ Thrust (sea level) to Weight (takeoff) Ratio')
%************************************
%************************************

% Mission 7 Service Ceiling at 65,000 ft

figure
WtoS = [0:1:nPts];

Ceiling1 = zeros(nPts);
for WtS = 1:nPts
   Ceiling1(WtS) = (0.187*K1^2*WtS) + 4.302/WtS ;
end

hold
plot(Ceiling1)
hold
axis([0,nPts,0,TtoWMax])
title('Service Ceiling')
xlabel('Wto/S ~ Wing Loading (takeoff) ~ lbf/ft^2')
ylabel('Tsl/Wto ~ Thrust (sea level) to Weight (takeoff) Ratio')


% Mission 8 Instantaneous Turn at 30k ft @ 6g's

figure
InsTurnWtoS = 171.4;
plot([InsTurnWtoS InsTurnWtoS],[0 TtoWMax])
axis([20,nPts,0,TtoWMax])
title('Instantaneous Turn Rate Performance')
xlabel('Wto/S ~ Wing Loading (takeoff) ~ lbf/ft^2')
ylabel('Tsl/Wto ~ Thrust (sea level) to Weight (takeoff) Ratio')

% Mission 9 Landing

figure
WtoS = [0:1:nPts];

Landing1 = zeros(nPts);
for WtS = 1:nPts
   Landing1(WtS) =  0.00083*WtS;
end

hold
plot(Landing1)
hold
axis([0,nPts,0,TtoWMax])
title('Landing')
```

```
xlabel('Wto/S ~ Wing Loading (takeoff) ~ lbf/ft^2')
ylabel('Tsl/Wto ~ Thrust (sea level) to Weight (takeoff) Ratio')


% Constraint Analysis Plots
figure
hold
plot(TakeOff1,'r')
text(nPts, TakeOff1(nPts),'Take Off')
plot(Casc1,'k')
text(nPts, Casc1(nPts), 'Cruise')
plot(SusTurn1,'c')
text(nPts, SusTurn1(nPts), 'Sus-Turn')
plot(MaxV1,'g')
text(nPts, MaxV1(nPts), 'Max Spd')
plot(Accel1,'m')
text(nPts, Accel1(nPts), 'Accel')
plot(Ceiling1, 'b')
text(nPts, Ceiling1(nPts), 'Svc Ceiling')
plot([InsTurnWtoS InsTurnWtoS],[0 TtoWMax],'b')
text(ceil(InsTurnWtoS), TtoWMax-.2, 'Inst Turn')
plot(Landing1, 'r')
text(nPts, Landing1(nPts), 'Ldg')


hold
axis([10,nPts,0,TtoWMax])
grid
title('UAV Constraint Diagram')
xlabel('Wto/S ~ Wing Loading (takeoff) ~ lbf/ft^2')
ylabel('Tsl/Wto ~ Thrust (sea level) to Weight (takeoff) Ratio')
```

APPENDIX C: ROUGH ORDER OF MAGNITUDE (ROM) ANALYSIS

The aircraft performance equations below are taken from Anderson [Ref. 26] and Hale [Ref. 27] and used in the evaluation of ROM analyses and in QFD Matrix 1. These equations are used with the performance data shown in Chapter III of this thesis. The results are then shown in Table 2 which shows the ROM impact on the HALE UAV customer attributes by each performance parameter. Three sample calculations of the ROM using the Endurance, Range and Cruise Altitude equation is shown after the following equations.

- $C_D = C_{D,O} + \dfrac{C_L{}^2}{\pi e AR}$
- $T_R = \dfrac{W}{L/D}$
- $(R/C)_{\max} = 600\left[\dfrac{(T/W)^3 (W/S)}{C_{D,0}}\right]^{1/2} = 600\left[\dfrac{T^3}{W^2 S C_{D,0}}\right]^{1/2}$
- $R = 2\dfrac{\sqrt{2}}{\sqrt{\rho_\infty S}}\dfrac{1}{C_t}\dfrac{C_L{}^{1/2}}{C_D}(W_O{}^{1/2} - W_1{}^{1/2})$ OR $R = \dfrac{25 w_f}{C_t}\left[\dfrac{1}{(W/b)\sigma}\right]^{1/2}\left[\dfrac{e}{(SC_{D,0})^3}\right]^{1/4}$
- $E = \dfrac{1}{C_t}\dfrac{C_L}{C_D}\ln\dfrac{W_O}{W_1}$ OR $E = \dfrac{0.886(W_f/W)}{C_t}\left[\dfrac{eAR}{C_{D,0}}\right]^{1/2}$
- $h_{\max ceiling} = 30500 \ln\left[0.866(T/W)\left[\dfrac{eAR}{C_{D,0}}\right]^{1/2}\right]$
- $S_{LO} = \dfrac{1.44W^2}{g\rho_\infty S C_{L,\max}\{T - [D + \mu_r (W - L)]_{ave}\}}$ OR $S_{LO} = \dfrac{20(W/S)}{\sigma(T/W)C_{L,\max}}$
- $n = \dfrac{L}{W} = \dfrac{1}{2}\rho_\infty V_\infty{}^2 \dfrac{C_{L,\max}}{W/S}$
- $\omega = \dfrac{gn}{V\infty} = g\sqrt{\dfrac{\rho_\infty C_{L,\max} n_{\max}}{2(W/S)}}$ OR $\omega = 100\left[\dfrac{eAR(T/W)}{(W/S)}\right]^{1/2}$

- $$V_{max} = \left[\frac{\left(\frac{T_A}{W}\right)_{max}\left(\frac{W}{S}\right) + \left(\frac{W}{S}\right)\sqrt{\left(\frac{T_A}{W}\right)^2_{max} - \frac{4C_{D,0}}{\pi eAR}}}{\rho_\infty C_{D,0}} \right]^{1/2}$$ OR $$V_{max} = 20\left[\frac{(T/W)(W/S)}{C_{D,0}}\right]$$

1. ENDURANCE

The Endurance relationship with regards to the performance parameters order of magnitude sample analysis is shown.

From Anderson [Ref. 26], we have, for maximum endurance:

$$E_{max} = \frac{1}{C_t}\left(\frac{C_L}{C_D}\right)_{max} \ln\frac{W_O}{W_1} = \frac{1}{0.6}(33.31)\ln\frac{25{,}600}{10{,}900} = \underline{\mathbf{47.4\ hours}}$$

Take the impact of fuel consumption of 0.6 lb fuel / lb thrust (see Chapter III, paragraph B-12);

$$\frac{1}{C_t} = 1 / 0.6 = 1.67 \ ;$$

Take the impact of $\left(\frac{C_L}{C_D}\right)_{max}$;

$\left(\frac{C_L}{C_D}\right)_{max} = 33.31$ (see Chapter III, paragraph B-8);

Take the impact of aircraft gross weight;

$\ln\frac{W_O}{W_1} = 25{,}600 / 10{,}900 = 0.55$; (see Chapter III, paragraph B-2);

The writer mentioned earlier that the known information about Global Hawk is used as a baseline reference in developing the HALE UAV design template discussed herein. It is noted that the HALE UAV endurance shown above is in broad agreement to the Global Hawk's endurance of 40 hours.

2. RANGE

The Range relationship with regards to the performance parameters order of magnitude sample analysis is shown.

From Hale [Ref.27], we have

$$R = \frac{25 w_f}{C_t}\left[\frac{1}{(W/b)\sigma}\right]^{1/2}\left[\frac{e}{(SC_{D,0})^3}\right]^{1/4}$$

Take the impact of $C_{D,0}$ (see Chapter III, paragraph B-12);

$$\left(\frac{1}{(C_{D,0})^3}\right)^{1/4} = \left(\frac{1}{(0.0161)^3}\right)^{1/4} = 22.12$$

Take the impact of Wing Loading (W/S) from the rearranged Range equation suggested by Hale [Ref. 27] to:

$$R = \frac{25 w_f}{C_t}\left[\frac{\frac{W}{S}}{\sigma}\right]^{1/2}\left[\frac{eAR}{(C_{D,0})^3}\right]^{1/4}$$

$$\left(\frac{W}{S}\right)^{1/2} = 40^{1/2} = 6.32$$

Take the impact of AR = 25 (see Chapter III, paragraph B-5);

$25^{1/4} = 2.24$

Take the impact of aircraft gross weight of 25,600 lbs (see Chapter III, paragraph B-2) ;

$$\frac{1}{\sqrt{W}} = \frac{1}{\sqrt{25600}} = 6.25\times10^{-3}$$

3. CRUISE ALTITUDE

The Cruise Altitude relationship with regards to the performance parameters order of magnitude sample analysis is shown.

From Hale [Ref.27], we have

$$h_{\max ceiling} = 30500 \ln\left[0.866(T/W)\left[\frac{eAR}{C_{D,0}}\right]^{1/2}\right]$$

Take the impact of T/W (see Chapter III, paragraph E);

T/W = 0. 33

Take the impact of AR = 25 (see Chapter III, paragraph B-5);

$\sqrt{AR} = \sqrt{25} = 5$

Take the impact of $C_{D,0} = 0.0161$ (see Chapter III, paragraph B-7);

$$\left(\frac{1}{C_{D,0}}\right)^{1/2} = 7.88$$

Take the impact of aircraft gross weight of 25,600 lbs (see Chapter III, paragraph B-2) ;

$$\frac{1}{W} = \frac{1}{25{,}600} = 3.9\times10^{-5}$$

APPENDIX D: MATLAB PROGRAM (VARIATIONS OF ACCELERATION)

This MATLAB code in Appendix D is to explore the impact of AR and $C_{D,0}$ on the acceleration performance curve in the constraint diagram.

```
% Acceleration Analysis
% Maj Rendell Tan - Thesis
clear all
%************************************
% Constants
% Maximum Thrust to Weight for Charts
TtoWMax = .5;

% Create Test Values for CDO
CDO1 = 0.0161;
CDO2 = 0.01288;

% Create Test Values for AR
AR1 = 25;
AR2 = 30;

% Wing Loading Test Values
nPts = 50;
WtoS = [0:1:nPts];
%************************************
%Examine Acceleration Performance

% Vary only AR by 120%
Accel1 = zeros(nPts);
for WtS = 1:nPts
   Accel1(WtS) = (0.0955*WtS)/AR2 + (355*CDO1)/WtS + 0.035;
end

% Vary only CDO by 80%
Accel2 = zeros(nPts);
for WtS = 1:nPts
   Accel2(WtS) = (0.0955*WtS)/AR1 + (355*CDO2)/WtS + 0.035;
end

% Original Equation
Accel3 = zeros(nPts);
for WtS = 1:nPts
   Accel3(WtS) = (0.0955*WtS)/AR1 + (355*CDO1)/WtS + 0.035;

end

%************************************
% Plotting Figures

figure
```

```
hold
plot(Accel1,'r')
text(nPts, Accel1(nPts),'120% AR')
plot(Accel2,'c')
text(nPts, Accel2(nPts), '80% CDO')
plot(Accel3,'b')
text(nPts, Accel3(nPts), 'Nominal')
hold
axis([10,nPts,0.25,TtoWMax])
grid
title('Acceleration Constraint Diagram with Nominal AR = 25, CDO =
0.0161')
xlabel('Wto/S ~ Wing Loading (takeoff) ~ lbf/ft^2')
ylabel('Tsl/Wto ~ Thrust (sea level) to Weight (takeoff) Ratio')
```

LIST OF REFERENCES

1. Cohen, Lou, *Quality Functional Deployment – How to Make QFD Work for You*, Addison-Wesley Publishing Company, Inc., Reading, Massachusetts, 1995.

2. Bossert, James L., *QFD – A Practitioner's Approach*, ASQC Quality Press, Milwaukee, Wisconsin, 1991.

3. Bicknell, Barbara A. and Bicknell, Kris D., *The Road Map to Repeatable Success – Using QFD to Implement Change*, CRC Press Inc., Boca Raton, Florida, 1995.

4. Akao, Yoji, *QFD – Integrating Customer Requirements into Product Design*, Productivity Press, Cambridge, Massachusetts, 1990.

5. Hauser, R. John and Clausing, Don, *The House of Quality,* Harvard Business Review, May-June 1988.

6. Head Quarters US Atlantic Command, *HAE UAV Joint Employment Concept of Operations*, July 1998.

7. Office of the Under Secretary of Defense, *Acquisition & Technology, Annual Report, Unmanned Aerial Vehicles (UAVs)*, August 1997.

8. Kopra, L. Timothy et al, *Application of a Concurrent Engineering Methodology to the Design of a Dual Use VTOL Aircraft*, American Institute of Aeronautics and Astronautics 94-4329-CP, 5th AIAA/USAF/NASA/ISSMO Symposium on Multidisciplinary Analysis and Optimization, Panama City Beach, Florida, 7-9 September 1994.

9. Johnson, C. Jon, *Advanced Lightweight Aircraft Fuselage Structure – Phase I*, SAWE Paper No. 2341, 55th Annual Conference of Society of Allied Weight Engineers, Inc., Atlanta, Georgia, 2-6 June 1996.

10. Wille, R.H., *Landing Gear Weight Optimization Using Taguchi's Analysis*, SAWE Paper Number 1966, Category Number 11, 49th Annual International Conference of Society of Allied Weight Engineers, Inc., Chandler, Arizona, 14-16 May 1990.

11. Lin, Paul and Jules, Kenol, *Optimized Multidisciplinary System Design for Aircraft and Propulsion Systems*, American Institute of Aeronautics and Astronautics 98-3265, 34th AIAA/ASME/SAE/ASEE Joint Propulsion Conference and Exhibit, Cleveland, Ohio, 13-15 July 1998.

12. Barnett, B.J. et al, *A Framework for Design Traceability*, Proceedings of the Human Factors Society, 36th Annual Meeting, 1992.

13. Benjamin, D.C., *Performance Study for Inlet Installations*, NASA-CR 189714, 1992.

14. Olds, John Robert, *Multidisciplinary Design Techniques Applied to Conceptual Aerospace Vehicle Design*, NASA-CR-194409, 1993.

15. Georgia Institute of Technology, *Integrated Design and Manufacturing for the High Speed Civil Transport*, NASA USRA Advanced Design Program Aeronautics, NASA-CR-197183, June 1994.

16. Scanlan, J.P, et al, *Modeling the Design Process within the Aerospace Industry*, Factory 2000-Advanced Factory Automation, Fourth International Conference, Publication 398, October 1994.

17. Gaffney, K.S. and Morones, P., *Advanced-Aircraft Integrated-Diagnostics System Concept Evaluation,* Reliability and Maintainability Symposium Annual Proceedings, 24-27 January 1994.

18. Dean, E.B., *Quality Functional Deployment for Large Systems, Engineering Management Conference*, 25-28 October 1992

19. Pohl, E., Robison, D., and Jacobs, J., *System Design with Quality Engineering, Aerospace and Electronics Conference*, 22-26 May 1989.

20. Doukas, L., Parkins, W. and Jeyaratnam, C., *Integrating Quality Factors into System Design,* Engineering Management Conference, 1995, Global Engineering management: Emerging Trends in the Asia Pacific, Proceedings of 1995 IEEE Annual International, 25-28 June 1995.

21. Tran, Tuyet-Lan, *QFD Application to a Software-Intensive System Development Project*, IEMC, 1996.

22. Reed, B.M., Jacobs, D.A. and Dean, E.B., *Quality Function Deployment: Implementation Considerations for the Engineering Manager*, Engineering Management Conference 1994, Management in Tranistion: Engineering a Chaing World, Proceedings of the 1994 IEEE International, 17-19 October 1994.

23. Beskow, C., Johansson, J. and Norell, M., *Implementation of QFD: Identifying Success Factors,* Engineering and Technology Management, IEMC '98, 11-13 October 1998.

24. Corban, R. Robert, *NTP System Definition and Comparison Process for SEI*, American Institute of Physics, Conference 930103, 1993.

25. Abbott, I. H. and Von Doenhoff A. E., *Theory of Wing Sections,* Dover Publications, Inc, New York, New York, 1959.

26. Anderson, J. D. Junior, *Introduction to Flight, 4th Edition*, John Wiley and Sons, San Francisco, California, 1999.

27. Hale, F. J., *Aircraft Performance, Selection, and Design*, John Wiley and Sons, New York, New York, 1984.

28. Mattingly, J. D., Heiser, W. H. and Daley, D. H., *Aircraft Engine Design,* American Institute of Aeronautics and Astronautics Education Series, New York, New York, 1987.

29. Discussions with Faculty Members, Aeronautical Department, Naval Postgraduate School, Monterey, California, 1999.

30. Nicolai, L. M., *Fundamentals of Aircraft Design*, METS Inc., San Jose, California, 1984.

31. Roskam, J., *Airplane Design*, Roskam Aviation and Engineering Corporation, Ottawa, Kansas, 1985.

32. Callister, W. D. J., *Materials Science and Engineering – An Introduction*, Fourth Edition, John Wiley and Sons, New York, New York, 1997.

33. Resetar, S. A., Rogers, J.C. and Hess, R.W., *Advanced Airframe Structural Materials – A Primer and Cost Estimating Methodology*, RAND R-4016-AF, Santa Monica, California, 1991.

34. Raymer, D. P., *Aircraft Design: A Conceptual Approach*, Third Edition, American Institute of Aeronautics and Astronautics Education Series, Reston, Virginia, 1999.

35. Bralla, J. G., *Design for Manufacturing Handbook*, Second Edition, McGraw-Hill, New York, New York,1998.

36. Author's field trip to the F-18 C/D Manufacturing Plant in Los Angeles, California, U.S.A., January 1999.

37. Kalpakjian, S., *Manufacturing Engineering and Technology*, Third Edition, Addison-Wesley Publishing Company, Reading, Massachusetts, 1995.

38. Strong, A. D., *Fundamentals of Composites Manufacturing: Materials, Methods and Applications*, Society of Manufacturing Engineers, Dearborn, Michigan, 1989.

39. Schwartz, M., *Composite Materials Handbook*, Second Edition, McGraw-Hill, Inc., New York, New York, 1992.

40. Blanchard, B. S. and Fabrycky W. J., *Systems Engineering and Analysis*, Third Edition, Prentice Hall International (UK) Limited, London, 1997.

This page is intentionally left blank.

INITIAL DISTRIBUTION LIST

1. Defense Technical Information Center 2
   8725, John J. Kingman Rd., STE 0944
   STE 0944
   Ft. Belvoir, VA 22060-6218

2. Head Librarian 2
   Defense Technology Towers Library
   1 Depot Road, #02-01, Defense Technology Tower A
   Singapore 109681

3. Dudley Knox Library 2
   Naval Postgraduate School
   411 Dyer Rd.
   Monterey, CA 93943-5101

4. Prof. Max F. Platzer 1
   Chairman, Department of Aeronautics and Astronautics
   Naval Postgraduate School
   Monterey, CA 93943-5106

5. Prof. Conrad F. Newberry 3
   Department of Aeronautics and Astronautics
   Naval Postgraduate School
   Monterey, CA 93943-5106

6. Mr. Richard A. Smith 1
   Program Manager, AFRL/SNRW Building 620
   2241 Avionics Circle Room N3F10
   Wright-Patterson AFB, OH 45433-7333

7. CDR Osa E. Fitch 1
   Code 40T, Naval Air Systems Command, Building 2109
   Unit 5 Suite 122, 48150 Shaw Road, Unit 5
   Paxtuxent River, MD, 20670-1907

8. Air Logistics Department, HQ Republic of Singapore Air Force 2
   Attn: MAJOR Rendell Kheng Wah Tan
   AFPN 8060, 303 Gombak Drive, #01-31
   Singapore 669645